(1)

ARMY RESEARCH LABORATORY

Flamespreading in Granular Solid Propellant: Initial Results

Douglas E. Kooker
Stephen L. Howard
Lang-Mann Chang

ARL-TR-446 June 1994

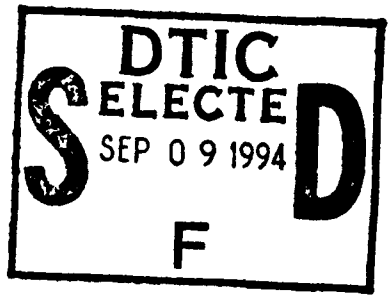

NOTICES

Destroy this report when it is no longer needed. DO NOT return it to the originator.

Additional copies of this report may be obtained from the National Technical Information Service, U.S. Department of Commerce, 5285 Port Royal Road, Springfield, VA 22161.

The findings of this report are not to be construed as an official Department of the Army position, unless so designated by other authorized documents.

The use of trade names or manufacturers' names in this report does not constitute indorsement of any commercial product.

REPORT DOCUMENTATION PAGE

Form Approved
OMB No 0704-0188

1. AGENCY USE ONLY (Leave blank)	2. REPORT DATE	3. REPORT TYPE AND DATES COVERED
	June 1994	Final, Oct 91 - Oct 93

4. TITLE AND SUBTITLE

Flamespreading in Granular Solid Propellant: Initial Results

5. FUNDING NUMBERS

PR: 1L161102AH43

6. AUTHOR(S)

Douglas E. Kooker, Stephen L. Howard, and Lang-Mann Chang

7. PERFORMING ORGANIZATION NAME(S) AND ADDRESS(ES)

U.S. Army Research Laboratory
ATTN: AMSRL-WT-PA
Aberdeen Proving Ground, MD 21005-5066

8. PERFORMING ORGANIZATION REPORT NUMBER

9. SPONSORING/MONITORING AGENCY NAME(S) AND ADDRESS(ES)

U.S. Army Research Laboratory
ATTN: AMSRL-OP-AP-L
Aberdeen Proving Ground, MD 21005-5066

10. SPONSORING/MONITORING AGENCY REPORT NUMBER

ARL-TR-446

11. SUPPLEMENTARY NOTES

12a. DISTRIBUTION/AVAILABILITY STATEMENT

Approved for public release; distribution is unlimited.

12b. DISTRIBUTION CODE

13. ABSTRACT *(Maximum 200 words)*

This study is an experimental investigation into fundamental aspects of ignition and flamespreading in compacted granular solid propellant. The 76-mm-diameter dual-chamber laboratory apparatus was designed as a closed-volume simulator with an ignition source at one end to generate a gas-phase planar wave. Diagnostics include wall-mounted pressure gages to monitor the time-history of the pressure field, and fast-response Type S thermocouples mounted in special hollow steel holders. Concern about adequacy of the thermocouple response time in this transient flow field is addressed by comparing data from 1-mil-, 2-mil-, and 3-mil-diameter thermocouples.

The simulator is loaded with two granular solid propellants: the triple-base M30A1 and the LOVA nitramine composite M43. Under certain conditions, the granular bed of "insensitive" M43 ignites more readily than the granular bed of M30A1, which emphasizes an important concept: *Time to ignition is determined by competition between the "flow residence time" and the "characteristic time for chemical reaction."* For M43, chamber diagnostics indicate pressures of 2–3 MPa and gas-phase temperatures in the range of 800–1,200 K before combustion runs away. These conditions are compatible with speculation that "dark zone" flame chemistry is controlling delayed ignition in LOVA propellant.

14. SUBJECT TERMS

granular solid propellant, LOVA propellant, delayed ignition, flamespreading, fast response thermocouples, flow simulator, solid propellants, ignition

15. NUMBER OF PAGES

35

16. PRICE CODE

17. SECURITY CLASSIFICATION OF REPORT	18. SECURITY CLASSIFICATION OF THIS PAGE	19. SECURITY CLASSIFICATION OF ABSTRACT	20. LIMITATION OF ABSTRACT
UNCLASSIFIED	UNCLASSIFIED	UNCLASSIFIED	UL

INTENTIONALLY LEFT BLANK.

ACKNOWLEDGMENTS

The authors would like to thank M. B. Ridgely and T. E. Rosenberger of the U.S. Army Research Laboratory (ARL) for their special assistance to this program at the ARL Indoor Range facility. The authors are also grateful to H. A. McElroy of the Olin Ordnance Corporation who, under the provisions of an ARL-Olin unfunded study agreement, supplied the ball powder propellant used in the igniter chamber.

INTENTIONALLY LEFT BLANK.

TABLE OF CONTENTS

INTENTIONALLY LEFT BLANK.

LIST OF FIGURES

1. INTRODUCTION

During the early stage of the gun interior ballistic cycle, the crucial process is the propagation of an ignition or flame front through the packed bed of unburned propellant grains or sticks. Few concerns arise as long as the flamespreading process is rapid and reproducible. However, if the solid propellant happens to be difficult to ignite (e.g., low vulnerability propellant), or if the strength of the ignition system is marginal, significant delays can arise in the propagation of flame through the propellant bed. Delays in flamespreading often lead to combustion chamber conditions that promote large amplitude pressure waves (e.g., Horst 1983). Diagnosing and correcting anomalous behavior associated with ignition and flamespreading would be much easier with a better understanding of the entire process.

The convective ignition process in many gun systems is dominated by a three-dimensional flow field as the result of the combustion chamber geometry, a center-core igniter, a projectile base which protrudes into the chamber, ammunition in separate bags, etc. Under these conditions, it is difficult to examine fundamental aspects of the process when the event is accompanied by an anomalous time delay. The present study is a deliberate attempt to remove these complications by employing a laboratory device with simplified geometry which encourages combustion within a compacted granular bed to propagate essentially as a planar wave.

A primary focus of this investigation is directed toward low vulnerability propellants, often referred to as LOVA propellants. The reduced vulnerability to various hostile threats is often associated with (a) a higher threshold for thermal ignition and (b) slower burning rates at low pressure. However, these very properties can also create difficulties in the ignition sequence of the gun system as discussed, for example, by Horst (1983). Since in many ways, the propagation of a convective ignition front through a bed of granular energetic material is poorly understood, it is not surprising that theoretical descriptions in various interior ballistic models are rather elementary. As a result, the models have not had much success in predicting scenarios involving pronounced time delays associated with establishing combustion. A data base from the present experiment should be helpful in validating improved models.

A discussion of a number of previous experiments that address ignition of a single grain and compacted aggregates can be found in Kooker, Chang, and Howard (1992). An important departure from much of the previous work is that the current experiment is not intended to simulate a particular primer, or to evaluate the performance of a class of igniter materials. The objective here is to understand ignition and longitudinal flamespreading in a bed of granular gun propellant. Features of the design were first

discussed in Kooker, Chang, and Howard (1992). An attempt was made to design a closed-volume apparatus with an ignition source that generates a planar wave composed of gas-phase products only, and would permit the gas composition of the igniter gases to be altered. An ignition stimulus that includes condensed-phase products is known to be effective, but these condensed-phase products are difficult to describe in a theoretical model. The present design deliberately promotes an ignition stimulus comprised of gas-phase products, which should allow a data base generated from this experiment to be compared to interior ballistic model predictions. The chamber volume is closed (as opposed to a flow-through device) to simulate conditions in the gun combustion chamber that will trap and retain all pyrolysis products from the solid propellant. Finally, the ignition wave should have a rise time of 2–4 ms and maintain a pressure level within the range of 1–4 MPa for the purpose of recreating the marginal ignition environment suggested by the simulator experiments of Chang and Rocchio (1988).

The current chamber design shares several ideas with the early Penn State experiment which may be the first attempt to employ a *controlled* environment for studying convective ignition and flamespreading in a granular propellant bed (Kuo et al. 1976; Kuo and Koo 1977). Because of interest in small-caliber ammunition, the granular propellant was confined in a section of a 30-cal. rifle barrel. Ignition was accomplished by spark-igniting an H_2/O_2 mixture held in an adjacent chamber; combustion gases driven through a nozzle plate formed the igniter wave in the flow chamber. The time-history from the wall-mounted pressure transducers gave clear evidence of a steepening pressure front propagating through the chamber, which is an important result from this work. All data, however, were generated from a single granular propellant, and hence, it is not possible to draw general conclusions about many aspects of convective ignition.

Of particular interest in the present study are propellants with distinctly different low-pressure flame-zone characteristics, such as the LOVA solid propellant M43 (RDX, CAB and NC) and the triple-base propellant M30A1 (NQ, NC, and NG). Recall that for M43 in the pressure range up to 4 MPa, the visible final flame zone appears to stand above the propellant surface, separated by a "dark zone" (e.g., see discussion in Vanderhoff et al. [1992] and Miller [1992, 1993]). Double-base solid propellants also exhibit this characteristic. By contrast, in the same pressure range, M30A1 shows evidence of a vigorous visible flame zone at or close to the propellant surface (Miller 1993). The current authors feel that these differences in flame structure at low pressure could have a major influence on the behavior of the solid propellant in a convective ignition environment. The present study hopes to eventually unravel how the chemical decomposition process interacts with the fluid mechanics.

2. FLAMESPREADING CHAMBER EXPERIMENT

Figure 1 is a schematic of the dual chamber apparatus designed to meet the objectives stated in section 1. The operation is straightforward. A small quantity of ball powder is burned in the igniter chamber which is sealed by a diaphragm and a multiple-nozzle plate from the flow chamber which contains the sample granular material. When the diaphragm bursts, combustion gases initially confined in the igniter chamber are driven through the nozzle plate forming a planar wave of hot gases which propagates through the flow chamber. The rise time and strength of the ignition wave are functions of the amount of ball powder burned in the igniter chamber, the burst pressure of the diaphragm covering the nozzle plate, the size of the nozzle holes, etc. In the present series of experiments, the plastic liner (which permits cinematography through openings in the outer steel chamber) was replaced by a 12.7-mm-thick aluminum liner.

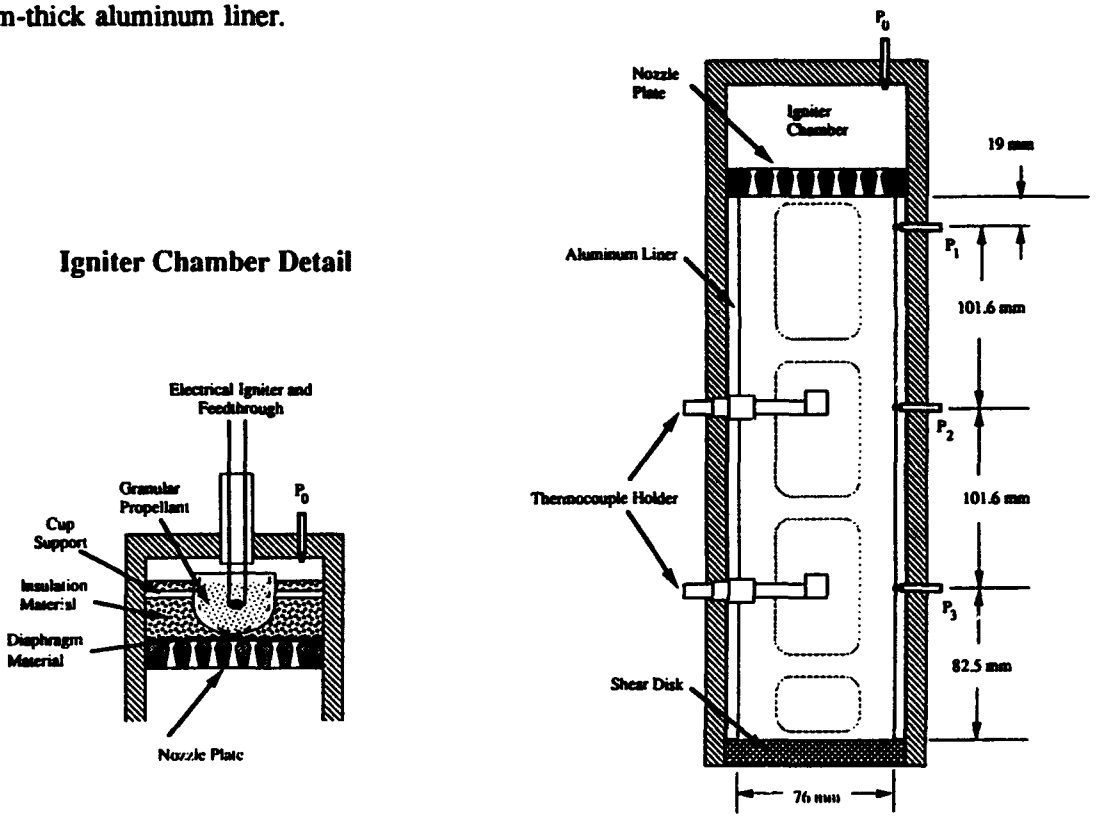

Figure 1. Schematic of flamespreading chamber apparatus with igniter chamber detail.

The inside diameter of the igniter chamber is 69.8 mm (2.75 in) and, in the present configuration, the length or height is 35 mm (1.375 in). However, various length internal sleeves can be used to adjust the height (hence, volume) as an additional control on the pressurization rate. A 12.7-mm-thick steel (0.5-in) nozzle plate with 101 holes (2.38-mm diameter) separates the igniter chamber from the flow chamber.

The flow chamber contains an aluminum liner with an inside diameter of 76 mm (3 in) and a length of 304.8 mm (12 in). A 9.5-mm-thick (0.375-in) acrylic blowout disc at the far end of the flow chamber limits the maximum chamber pressure. Pressure time-history of the chamber event is recorded by four wall-mounted Kistler 211B1 pressure transducers; P_0 is in the igniter chamber, and the other three are in the flow chamber, separated by 101.6 mm (4.0 in). P_1 is located 19 mm (0.75 in) into the flow chamber, P_2 is at 120.6 mm (4.75 in), and P_3 is at 222 mm (8.75 in).

The diaphragm covering the nozzle plate must retain its integrity while pressure builds in the igniter chamber and combustion of the ball powder is well under way. An additional problem is to prevent the burning ball powder from being entrained into the flow through the nozzle plate and, hence, entering the flow chamber to create a two-phase ignition environment. Figure 1 is a schematic of the current system. Typically, 5 g of Olin ball powder (undeterred sieved WC-870, average particle diameter of 0.775 mm) are placed within a 38-mm-diameter (1.5-in) aluminum "cup" and then ignited near the top with a bridge wire; to minimize heat loss, the cup is thermally insulated with a coating of white RTV. The diaphragm system is multi-layered. Pressure sealing is done by two thicknesses of mylar (~4 mil/sheet) which cover the nozzle plate. The other materials serve as a thermal shield to prevent hot ball powder particles, which might escape over the side of the cup, from prematurely burning through the mylar discs before they reach their burst pressure (two discs => ~16 MPa). Two layers of aluminum foil in the shape of a donut (inside diameter = 50.8 mm) are placed directly on top of the mylar discs. Then the aluminum cup is surrounded by another donut (inside diameter = 38 mm) of "furnace filter" material (spun glass wool) approximately 18 mm in height; this donut of filter material is covered on the top by a single layer of aluminum foil. These thermal layers are essentially consumed during the operation of the igniter chamber, hopefully with only a minimal contribution to the composition of the igniter gases.

To gain a better understanding of what happens during an anomalous ignition event, this chamber experiment will monitor static pressure and *temperature* of the gases within the packed granular bed. Measurement of gas temperature under these conditions is not a trivial task. The ignition event occurs within a time interval of a few milliseconds to several tens of milliseconds, but significant temperature changes can take place on a time scale of 1 ms. In addition, virtually any technique to measure gas temperature within the packed bed will locally disturb or alter the bed.

Of the temperature measurement options available (e.g., McClure [1984]), the choice here is to use a Type S thermocouple (platinum vs. platinum—10% rhodium) in a special holder. The maximum temperature limit of a Type S is approximately 2,040 K. Hence, it should provide an adequate history

of an ignition and/or incomplete combustion scenario which is the objective of this study. Of course, upon successful ignition, as the solid propellant grains transition to full combustion, the thermocouple will melt. A serious problem is how to protect the structural integrity of a thermocouple placed within the packed bed; all solutions involve compromise of some sort. The scheme adopted here (see Figure 1 and details in Figure 2) is to mount the thermocouple(s) inside a hollow steel cylinder which has dimensions similar to a typical solid propellant grain. In the current configuration, the hollow steel cylinder is rigidly mounted to the chamber wall. Allowing it to float with the motion of the packed bed creates major difficulties associated with maintaining wire connections and tracking position as a function of time. Two thermocouples may be mounted within each hollow steel cylinder, which has a diameter of 8 mm, a length of 11 mm, a wall thickness of 0.5 mm, with the axis of the cylinder held 34 mm from the chamber wall (which positions the thermocouple near the center of the packed bed). The experimental apparatus provides for two such thermocouple holders (see Figure 1), one located at the axial position of pressure transducer P2 and the other at P3. Each thermocouple is "strung across" an inside diameter of the hollow cylinder (like a clothesline) with the junction located near the cylinder axis; this configuration is held fixed by applying a coating of clear NC-based lacquer with polyester resin to the inside of the hollow cylinder, which also electrically insulates the thermocouple leads from the steel walls. The lead wires are fed through the ceramic insulator within the sting mount (see Figure 2) and then connected to the outside world. For additional information on deployment of the thermocouples, see Howard, Chang, and Kooker (1994).

TOP VIEW (Thermocouple Enlarged for Clarity)

ENLARGED PART - SECTION A-A

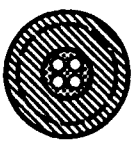

SIDE VIEW

Figure 2. Schematic of thermocouple holder.

Not yet addressed is the important question of evaluating response time of a thermocouple in a transient flow field. Although a characteristic time can be computed for a given thermocouple suddenly immersed in a constant-temperature stagnant or flowing gas field, these estimates are not reassuring when the situation involves fast transients. In the present authors' opinion, the only reasonable option is to evaluate a series of thermocouples with increasing sensitivity in the identical transient environment. The strategy adopted here was to mount two thermocouples of different diameters within the same holder, and compare the response from each one during a typical operation of the experiment. In each evaluation run, the chamber is filled with an inert "rubber-like" granular propellant simulant (see Table 1); the thermocouples then monitored gas temperature generated by the ignition wave within the inert packed bed. The general features of the ignition wave created when the diaphragm ruptures are illustrated by the pressure curve in Figure 3. Choked flow through the nozzle plate drives the initial pressure rise in a time interval of approximately 3 ms. When the nozzles unchoke, the pressure abruptly forms a plateau region (at approximately 2.5 MPa in Figure 3) with variations due to competition between heat loss (to the steel nozzle plate and to the initially cold propellant grains) and combustion of the remaining ball powder grains in the igniter chamber which drives the hot gas wave (see discussion of model results in Kooker, Chang, and Howard [1992]). The decay of pressure level during the 5–10 ms interval after unchoking is the result of heat losses exceeding combustion driving; as propellant grains and nozzle plate increase in temperature, the balance reverses which accounts for the slight increase in pressure level for the next 10 ms. Of course, heat loss eventually dominates the long-time behavior and the pressure decays. However, the experiment is able to hold gas pressure in a granular bed to within 20% of a constant level for over 50 ms.

Table 1. Properties of Solid Propellant Grains

Properties/Propellant	Inert Granular Simulant	M30A1 (7 Perf) (8-in Gun, XM188)	M43 (19 Perf)
Grain Length (mm)	24.3	28.5	13.9
Grain Diameter (mm)	10.7	12.3	8.43
Perf Diameter (mm)	0 (Solid Cylinder)	1.23	0.355
Density (g/cm^3)	~1.60	1.67	1.65

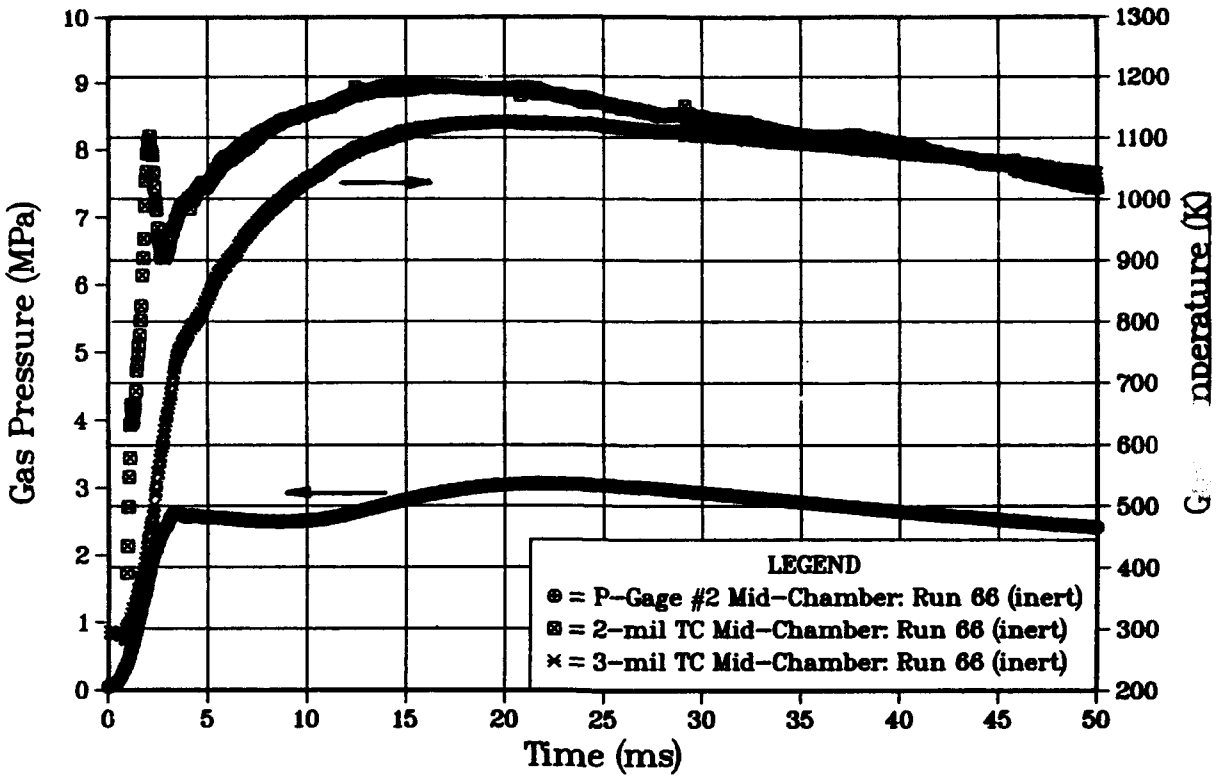

Figure 3. Comparison of temperature time-history from 2-mil and 3-mil thermocouples at mid-chamber location P2, along with pressure time-history at P2. Chamber contains granular inert simulant.

Type S thermocouples with three different diameters (1-mil, 2-mil, and 3-mil) were evaluated for response time. Figure 3 shows a 50-ms "window" of temperature time-history reported by a 2-mil and a 3-mil thermocouple, both of which are mounted within the same holder at "mid-chamber" (opposite P2), along with the pressure time-history from P2. Temperatures indicated on all the graphs are computed directly from the manufacturers' static calibration curve with no correction for radiation (our radiation calculations suggest a temperature correction of 10–30 K). Both thermocouples indicate an abrupt temperature rise just after the pressure transducer reports. However, the 3-mil thermocouple clearly lags the response of the 2-mil thermocouple during the important initial 25-ms time interval after passage of the ignition wave. (Note: the "mini-spike" reported by the 2-mil thermocouple in this run near a time of 3 ms may be an artifact—probably caused by the ubiquitous thermocouple gremlin). This response lag is responsible for an indicated temperature deficit of more than 200 K (during the initial 5-ms time interval). It is important to look for evidence that these indicated temperature differences are indeed the result of convective heat transfer to different diameter wires, and not spurious results of the measurement system. Figure 4 is an extended-time plot of the same temperature time-history displayed in Figure 3. The 2-mil thermocouple which reports higher temperatures up to a time of 40 ms, reports lower

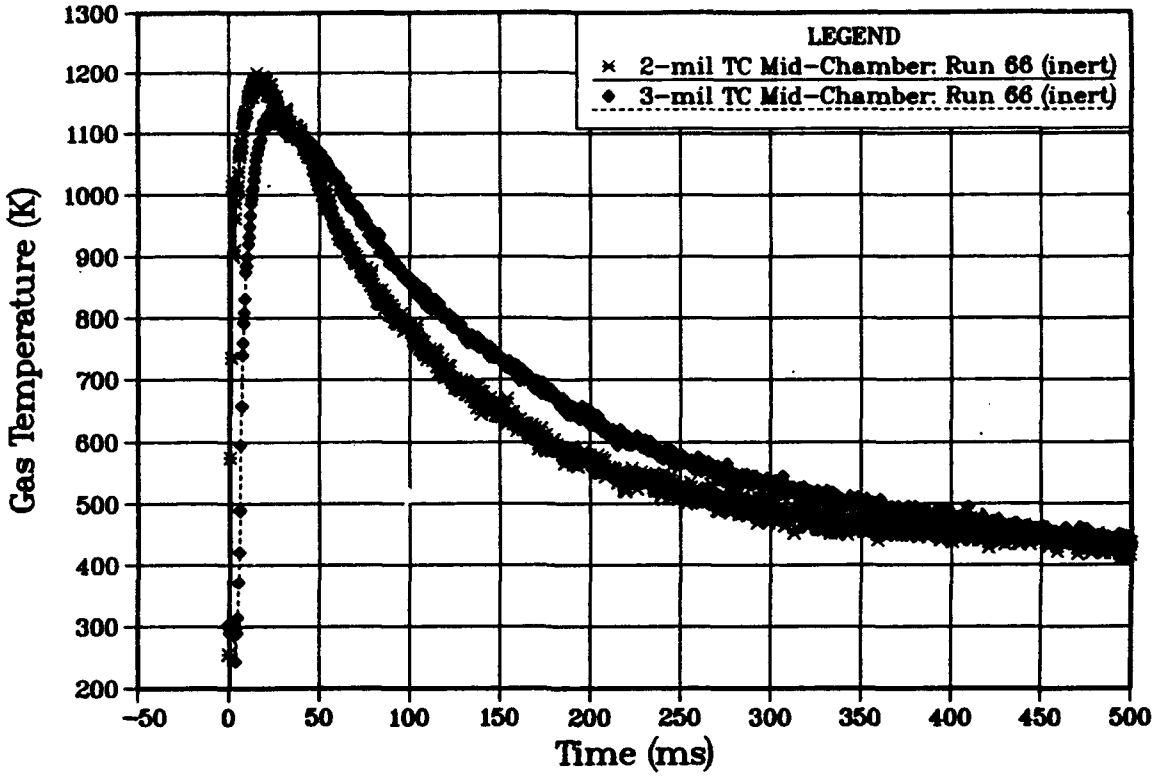

Figure 4. Comparison of temperature time-history from 2-mil and 3-mil thermocouples at mid-chamber location P2 over long time interval. Note thermocouple readings asymptotically approach the same temperature after 500 ms. Chamber contains granular inert simulant.

temperatures after that time until both thermocouple time-histories merge asymptotically at approximately 500 ms. This behavior is certainly compatible with higher heat transfer rates to the smaller diameter wire (2-mil) which would imply higher temperatures during a rapid heating phase and lower temperatures during a cooling phase. The thermocouples appear to behave in a rational manner. However, the slow response of the 3-mil thermocouple is judged to be unacceptable for this transient experiment.

The chamber firings discussed above were repeated but with a 1-mil and a 2-mil Type S thermocouple mounted in the mid-chamber thermocouple holder. Results from the initial [illegible]as time window are shown in Figure 5. As the temperature time-histories indicate, both thermocouples report the initial rise nearly inphase (on this time scale). However, at the 1,000 K level, the 2-mil thermocouple is clearly lagging the 1-mil, which continues to a peak of 1,300 K. The comparison shown in Figure 5 is the general trend: during the initial 5–10 ms, the 2-mil thermocouple can under-report the temperature by as much as 200 K (100–150 K is more typical), but after this initial time period, both thermocouples read within approximately 50 K of each other. On the basis of this comparison, the 1-mil thermocouple

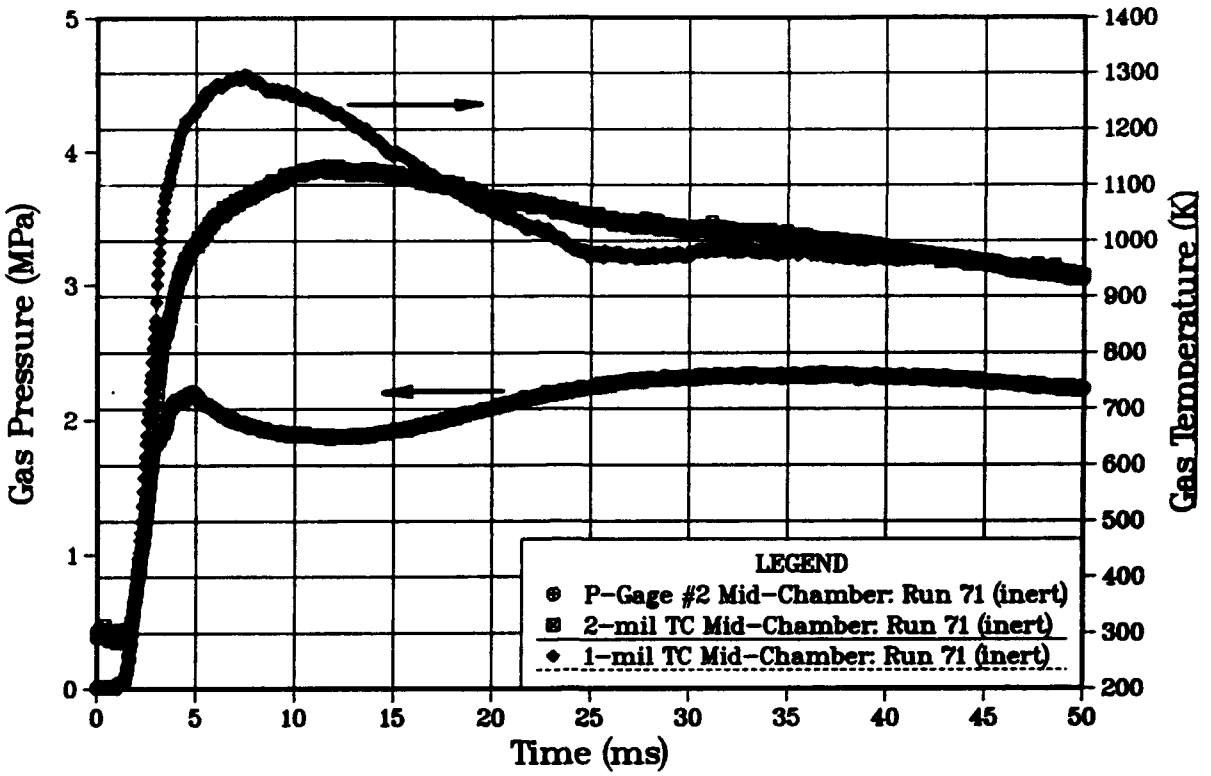

Figure 5. Comparison of temperature time-history from 1-mil and 2-mil thermocouples at mid-chamber location P2, along with pressure time-history at P2. Chamber contains granular inert simulant.

should be the choice. However, the issues of strength and delicacy of the 1-mil lead wires (and the additional time penalty associated with setup) forced a practical decision to proceed with 2-mil thermocouples in the remaining experiments. Thus, temperatures reported in subsequent runs from the 2-mil thermocouples should be viewed as minimum values (by possibly 200 K) in the important initial 10-ms time interval.

3. RESULTS WITH GRANULAR SOLID PROPELLANT

The evaluation phase with inert granular simulant described in section 2 provides important information about the ignition wave environment created in the chamber apparatus. Although several additional questions remain, time and funding constraints dictated that the experiment proceed to the live propellants, M30A1 and M43. With identical grain size, the ignition wave flow environment, at least for early time, should be nearly the same. This is indeed the goal for the final evaluation experiments, and will be possible by selecting 7-perf, equal-sized cylindrical grains from a special batch of research propellants (Miller 1992). For the present series of runs, however, no attempt was made to employ

equivalent grain size. The criteria here was based solely on availability, and, in fact, very diverse grain sizes were used (see Table 1). As will be seen later, this choice happens to illuminate an important aspect of "time-to-ignition."

3.1 M30A1 Granular Propellant. The M30A1 propellant is a large, cylindrical 7-perf grain taken from an XM188 charge for the 8-in gun. Two packed-bed configurations were tested in the flamespreading chamber. In the "full-up" configuration shown in Figure 6a, 1,138 g of propellant were loaded into the chamber to a level 19 mm below the nozzle plate (initial porosity was 0.475). The 19-mm void region is intended to keep the propellant grains out of the harsh supersonic/subsonic flowfield adjustment downstream of the choked nozzle exit plane. Even with this provision, there was concern that leading edge grains might be "torched" in an environment quite dissimilar to the rest of the bed. To examine this influence, a second configuration was constructed (see Figure 6b) by removing an 82.5-mm length of the propellant column and replacing it with a column of the inert granular simulant to form a packed-bed buffer zone between the nozzle exhaust region and the leading edge of the live propellant bed.

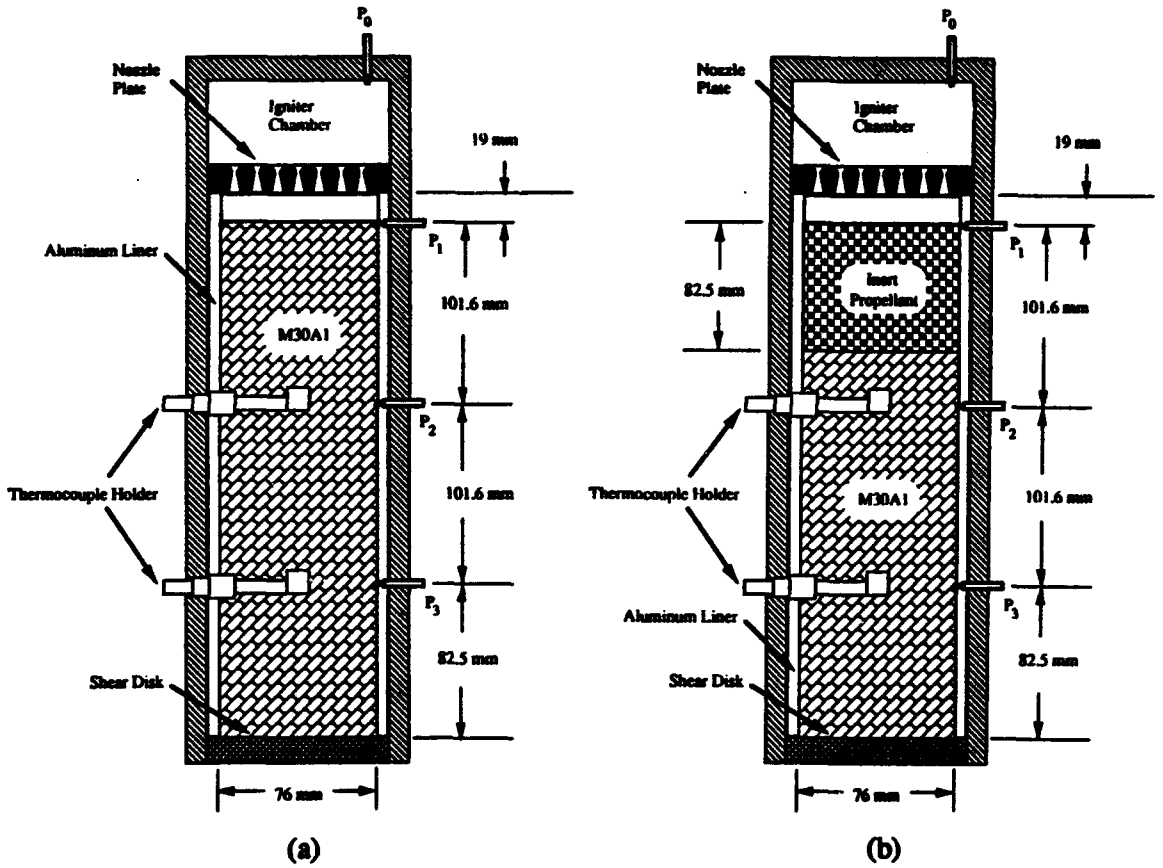

Figure 6. Schematic of chamber loading configurations used in tests of M30A1 propellant: (a) denoted "full-up" (no inert buffer zone) and (b) 82.5-mm length of inert buffer zone.

Figure 7 compares the pressure time-history (from the mid-chamber gage P2) from two tests with granular M30A1, in the configurations of Figure 6. The characteristics of the igniter-driven wave are nearly identical in both cases; the rise time is approximately 3 ms, leaving a pressure plateau at 2 MPa. Ignition is successful in both configurations, with the full-up case (Figure 6a) showing an induction time of 7–8 ms while the buffer-zone configuration (Figure 6b) indicates 12–13 ms. The rate of pressurization is slower in the latter case primarily because the same chamber volume contains less energetic material. In each run, gas-phase temperatures were reported by a 2-mil thermocouple. There are some important differences. The temperature time-history measured by the mid-chamber thermocouple (see Figure 8) in the 6a configuration strongly suggests that some type of exothermic reaction (e.g., propellant pyrolysis with incomplete energy release) accompanied the passage of the initial ignition wave. Unfortunately, this thermocouple signal may have been drifting because the indicated ambient temperature is 400 K (not correct). Furthermore, the thermocouple may have sustained some damage during the brief excursion to the region above 2,000 K, and hence the values reported as combustion runaway (near 15 ms) are suspicious. Figure 9 shows similar time-histories from a 2-mil thermocouple and wall-mounted pressure transducer for the 6b configuration. The time-histories illustrated in Figure 9a are from the mid-chamber location, and show a temperature rise from 300 K to approximately 1,200 K as the igniter-driven wave passes over. Note that this temperature rise is not as abrupt as that seen at mid-chamber in the full-up configuration. Then during the next 10 ms, the temperature continues to increase to 1,600 K before runaway is in full progress. Figure 9b illustrates a similar comparison between the 2-mil thermocouple and pressure transducer at location P3. At this depth into the bed, the temperature increase created by the igniter-driven wave is quite modest and only rises to less than 1,000 K before the strong combustion wave passes this location and blows the shear disc out of the chamber.

3.2 M43 Granular Propellant. The LOVA M43 propellant used here is a 19-perf cylindrical grain with dimensions (see Table 1) roughly half those of the M30A1 grain. In addition, the surface of the M43 grain is coated with a thin layer of graphite which seems to promote aggregate formation (packing into a bed) by reducing grain-to-grain friction forces. Apparently as a result, the initial bed porosity was found to be close to 0.40. At this porosity in the full-up chamber configuration, the total propellant weight would have exceeded the explosive weight limit of the test bay. Hence, the full-up configuration illustrated in Figure 10 shows a 38-mm layer of inert granular simulant at the chamber bottom. Two other configurations (only one of which is illustrated in Figure 10) include inert buffer zones adjacent to the nozzle plate, and hence, do not require the bottom layer of inert simulant.

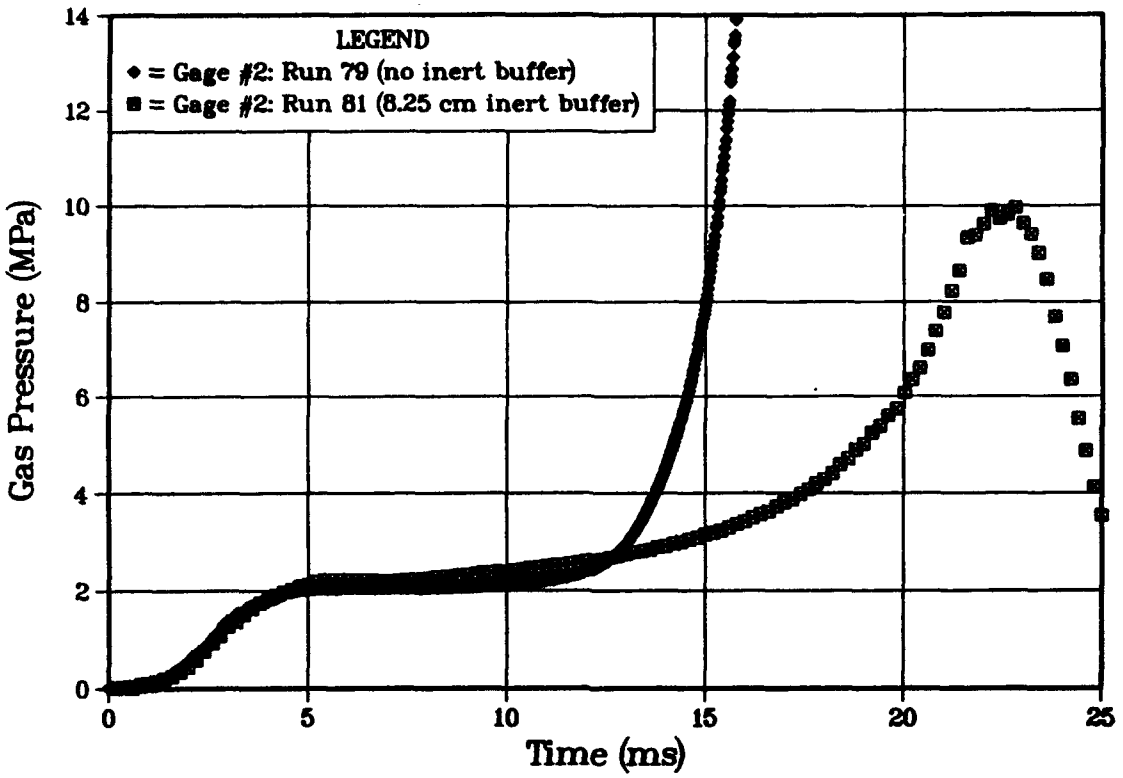

Figure 7. Comparison of pressure time-history location P2 for two chamber loading configurations containing granular M30A1 propellant: see Figures 6a and 6b.

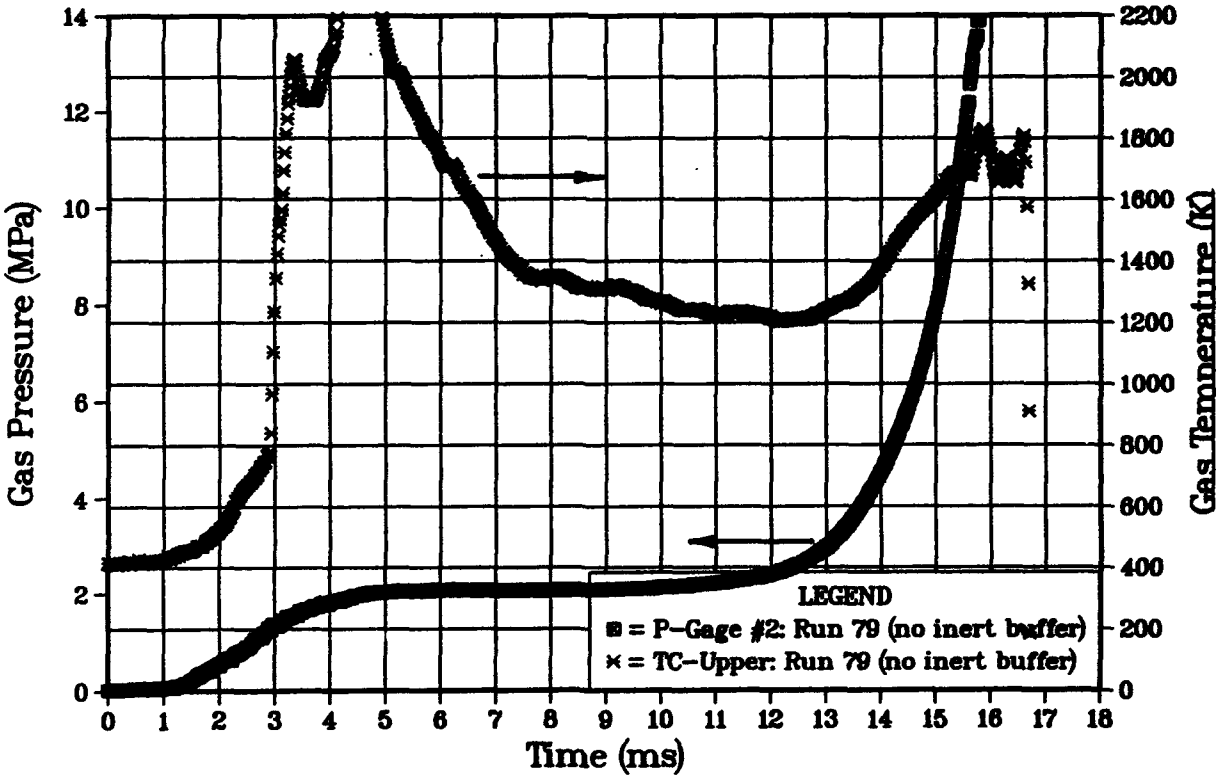

Figure 8. Comparison of temperature time-history from the 2-mil thermocouple and pressure time-history from the transducer at mid-chamber location P2. M30A1 loaded as in Figure 6a. Thermocouple signal may have been drifting; and thermocouple may have been damaged by the excursion beyond 2,000 K.

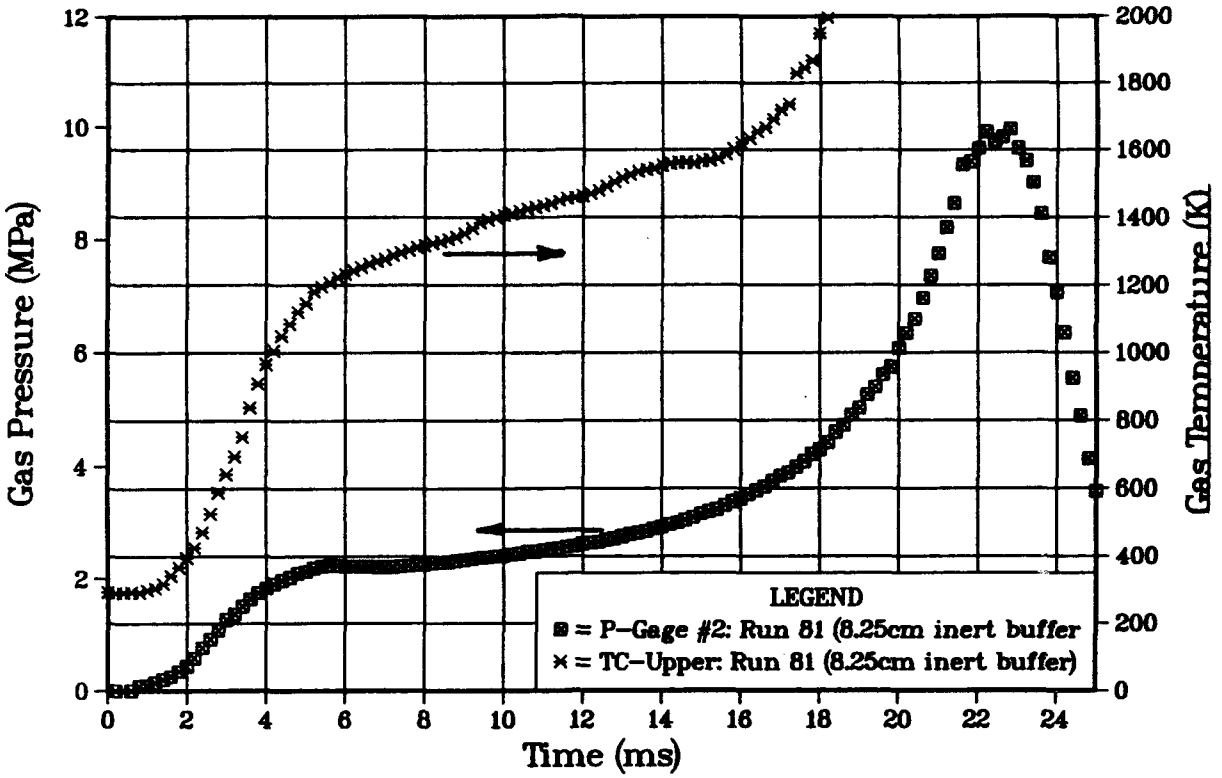

(a) Thermocouple and pressure transducer are both located at P2.

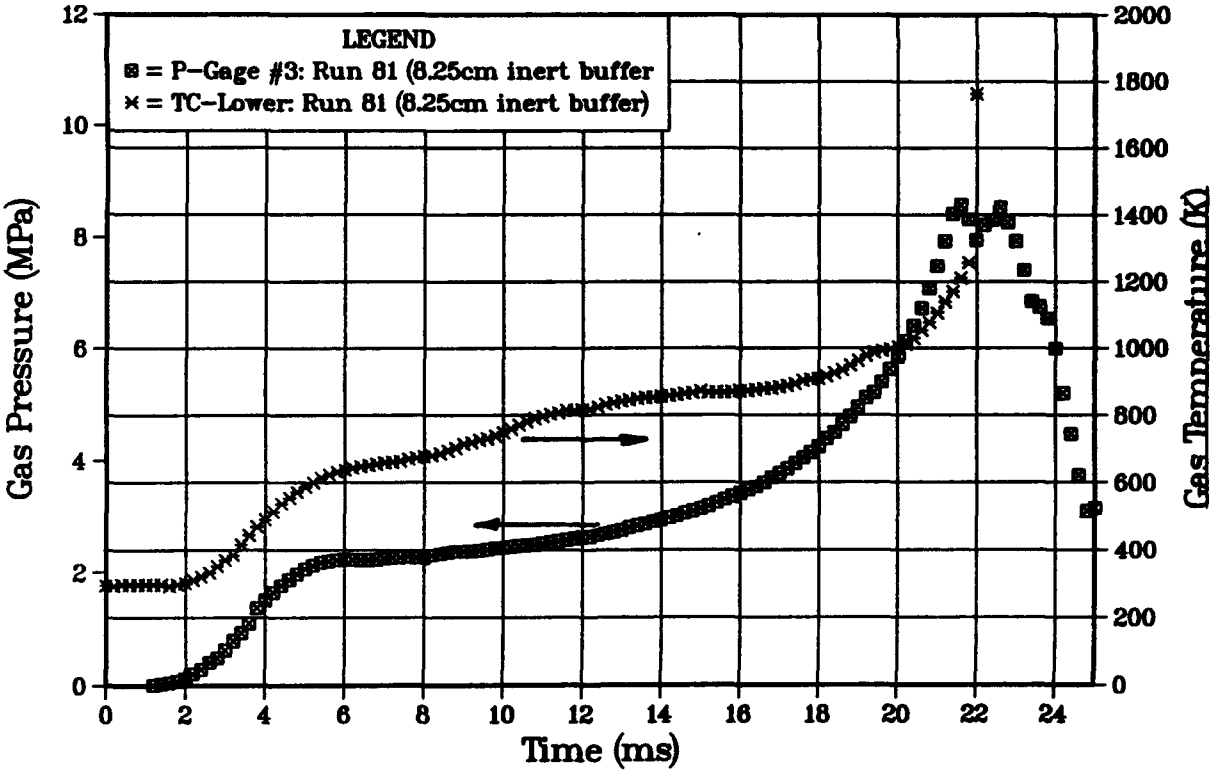

(b) Thermocouple and pressure transducer are both located at P3.

Figure 9. Comparison of temperature time-history from a 2-mil thermocouple and pressure time-history from the transducer for the M30A1 chamber loading configuration shown in Figure 6b.

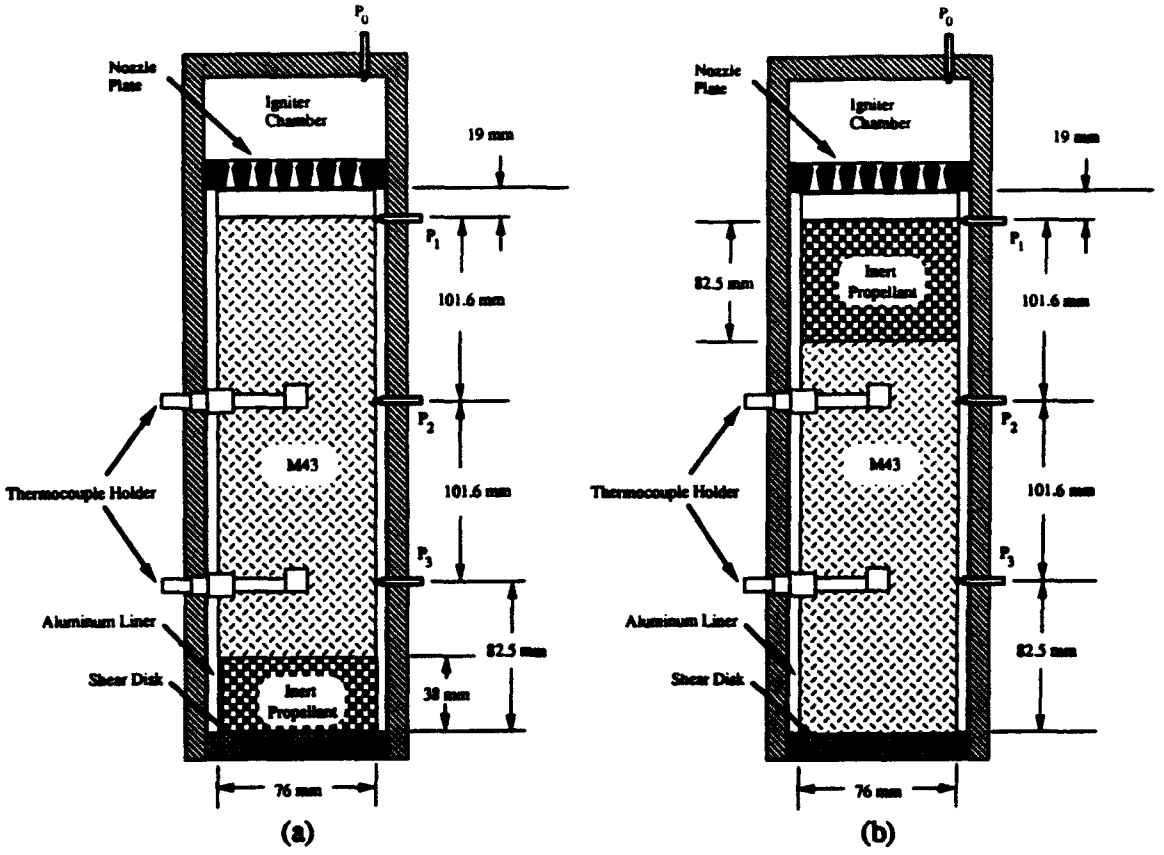

Figure 10. Schematic of chamber loading configurations used in tests of M43 LOVA propellant: (a) denoted "full-up" (no inert buffer zone) and (b) 82.5-mm length of inert buffer zone.

Figure 11 compares the pressure time-history (from the mid-chamber gage P2) from three tests containing granular M43: the 10a configuration (Figure 10a), a configuration with a 38-mm length of inert buffer zone (analogous to Figure 10b, but not illustrated), and the 10b configuration. Several interesting observations can be made here. The full-up configuration and the 38-mm inert buffer zone configuration both ignited successfully; the configuration with the 82.5-mm inert buffer zone failed to ignite. A surprising result is that "insensitive" M43 LOVA propellant in the full-up configuration shows virtually no induction time or ignition delay, but M30A1 in the same configuration (discussed above) exhibits a 7–8 ms delay. This counter-intuitive result makes more sense when examining the whole flow environment—particularly gas permeability of the packed bed. The bed formed by the small M43 grains is significantly less permeable than the bed formed by the large M30A1 grains. Given the same igniter stimulus located 19 mm away from the edge of the propellant bed, the rate of pressure increase will be much greater for the bed with low permeability. Hence, in the 10a configuration, the rapidly rising pressure field near the leading edge of the low-porosity M43 bed creates a very favorable environment for the ignition process—particularly for M43 which has shown some reluctance to ignite at lower pressures. The fact that, in this configuration, M43 propellant ignites more readily than M30A1 propellant

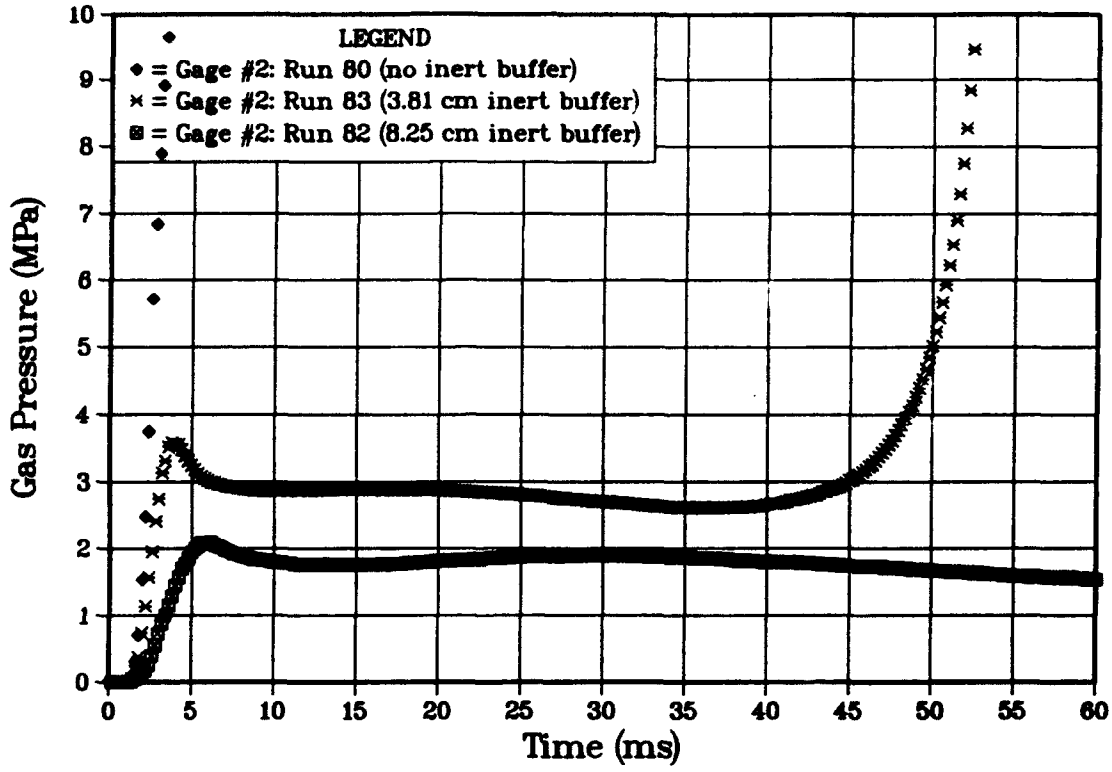

Figure 11. Comparison of pressure time-history at mid-chamber location P2 for three chamber loading configurations containing granular M43 propellant: no inert buffer zone (Figure 10a), 38-mm length of inert buffer zone (similar to Figure 10b), and 82.5-mm length of inert buffer zone (Figure 10b).

serves to emphasize a very important concept: *Time to ignition in a granular propellant bed is governed by competition between the "flow residence time" and the "characteristic time for chemical reaction" (the ratio being a Damkohler number).* The lower permeability of the M43 bed leads to a longer "flow residence time" while the rapidly rising pressure reduces the "characteristic time for chemical reaction". Although neither characteristic time has been determined here, the current results demonstrate that flow environment adjustments which increase flow residence time and/or shorten the chemical reaction time will decrease the time to ignition.

The pressure time-histories shown in Figure 11 provide a brief overview of the M43 behavior, but the experiments provided much additional information. For the run involving the full-up configuration, the 2-mil thermocouples at locations P2 and P3 both responded to the passing combustion wave by abruptly exceeding their maximum values (i.e., melting). However, the three wall-mounted pressure transducers easily witnessed the flame propagation event and reported the time-histories shown in Figure 12. The speed of flame propagation (based upon the time to attain the 2-MPa level) is approximately 162 m/s and nearly uniform through the chamber. Note that gage P3 senses rupture of the shear disc at a pressure level of approximately 9 MPa, and the resultant release wave halts the pressurization process.

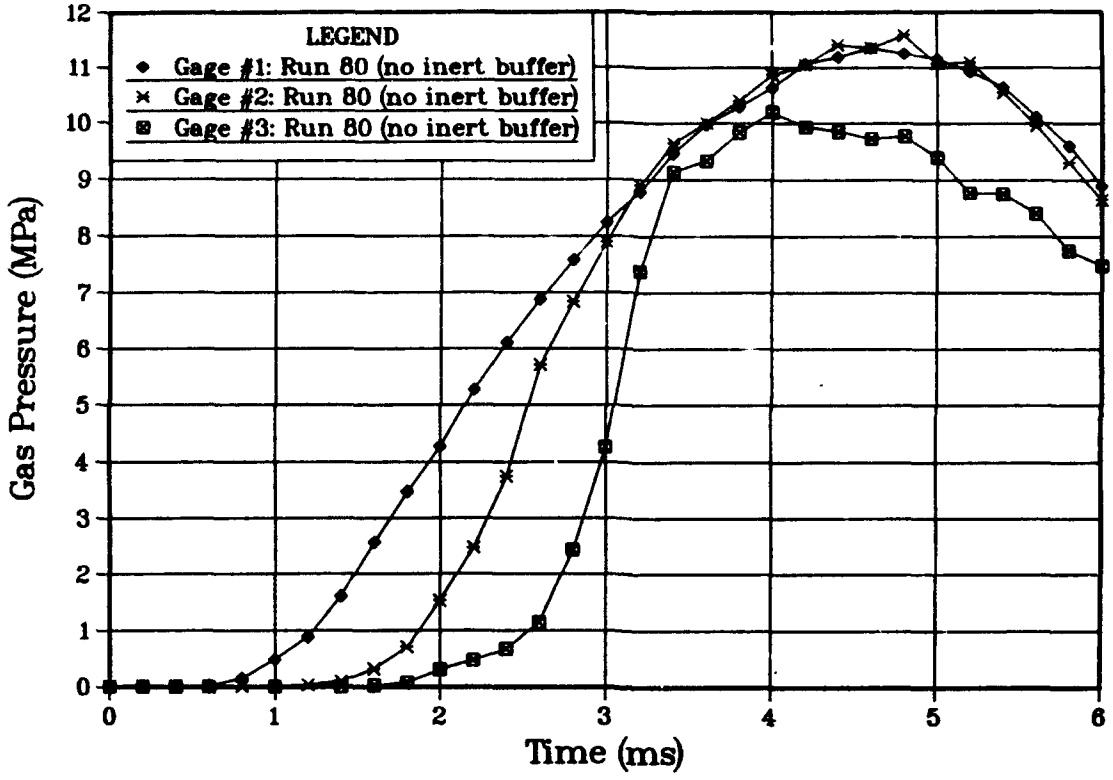

Figure 12. Comparison of pressure time-history at locations P1, P2, and P3 for the chamber loading configuration with no inert buffer zone (Figure 10a). Chamber contains M43 granular propellant. Flame propagates at approximately 162 m/s.

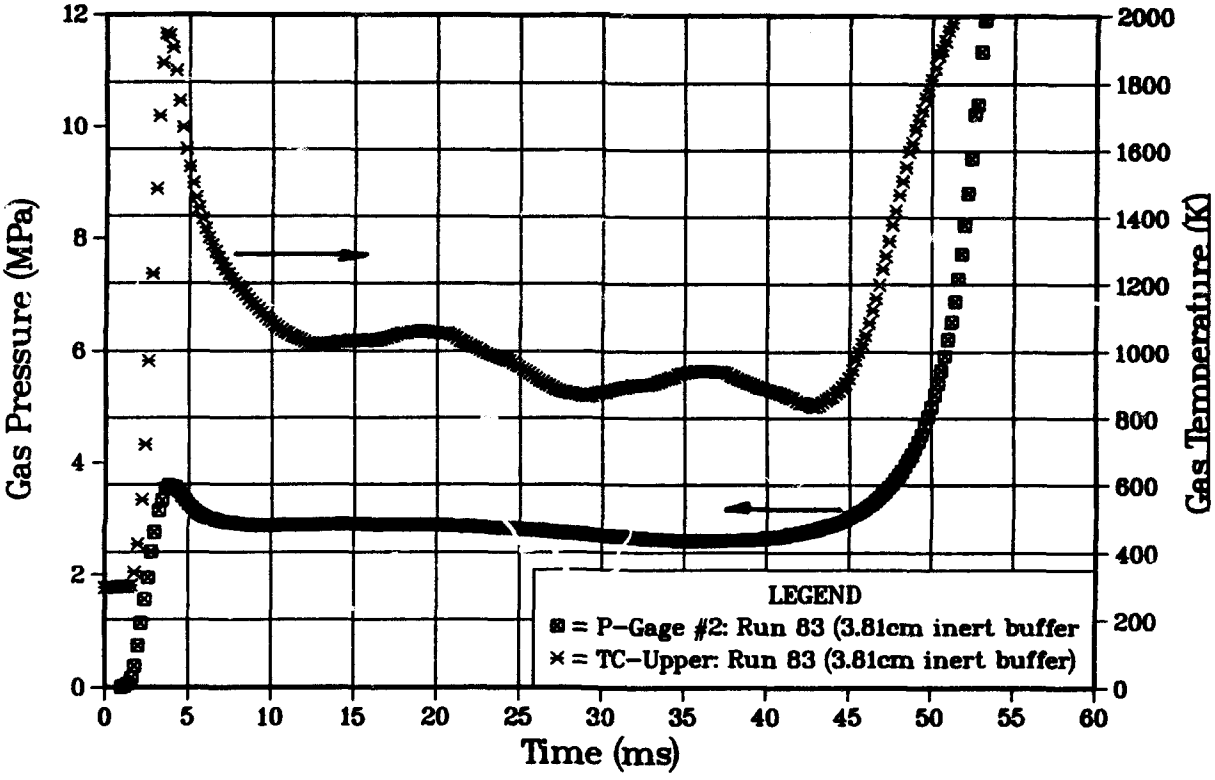

Figure 13. Comparison of temperature time-history from the 2-mil thermocouple and pressure time-history from the transducer at mid-chamber location P2. M43 propellant loaded into chamber with 38-mm inert buffer zone (similar to Figure 10b).

The M43 run based on the configuration with a 38-mm inert buffer zone produced a "hang-fire" ignition event with an induction time delay of more than 40 ms. Figure 13 compares the pressure time-history from P2 with the temperatures reported by a 2-mil thermocouple at the same location. Apparently the igniter wave induces some type of exothermic response from the propellant, since the thermocouple reports a gas temperature excursion to near 2,000 K. This response is quite similar to that exhibited by M30A1 in the full-up configuration (see Figure 8). In the present M43 run, as the gas pressure in the bed stabilizes near 3 MPa, the gas temperatures decline to 1,000 K and continue to decay toward 800 K (Note: the oscillations in temperature in Figure 13 are probably not physical, but are attributable to the interference of line noise [16.7 ms/cycle]). At approximately 43 ms, the combustion process, which has been hanging in the balance for 40 ms, roars to life as witnessed by both the thermocouple and pressure transducer.

The M43 run based on the 10b configuration (82.5-mm inert buffer zone) failed to ignite. Here, failure includes a 45-min waiting period during which gas temperature in the packed bed was monitored by the "in situ" thermocouples. It is important to emphasize a major effect of changing the length of the inert buffer zone ahead of this M43 granular bed. Since the grain size of the granular inert simulant is larger than the M43 propellant, increasing the length of the buffer zone adds a more porous section of bed adjacent to the igniter system. Assuming the igniter strength is unaltered, the igniter gases have a larger volume to expand into which lowers the pressure plateau level seen by the propellant bed. Note in the present case, increasing the buffer zone length from 38 mm to 82.5 mm lowers the pressure level from 3 MPa to 2 MPa. This change in pressure level could have a significant influence on the gas-phase chemical kinetic rates associated with decomposition schemes currently proposed for propellant dark zones (Vanderhoff et al. 1992). Gas-phase temperature time-history recorded by a 2-mil thermocouple at location P2 is shown over a 100-ms window in Figure 14 along with the corresponding pressure. Note that the gas temperature at mid-chamber reaches 1,100 K with the arrival of the igniter wave, but decays from that time on. At the lower location, the gas temperature (not shown in Figure 14) does not exceed 625 K. Again, note that the indicated temperature oscillations are most likely the result of line noise and hence not physical.

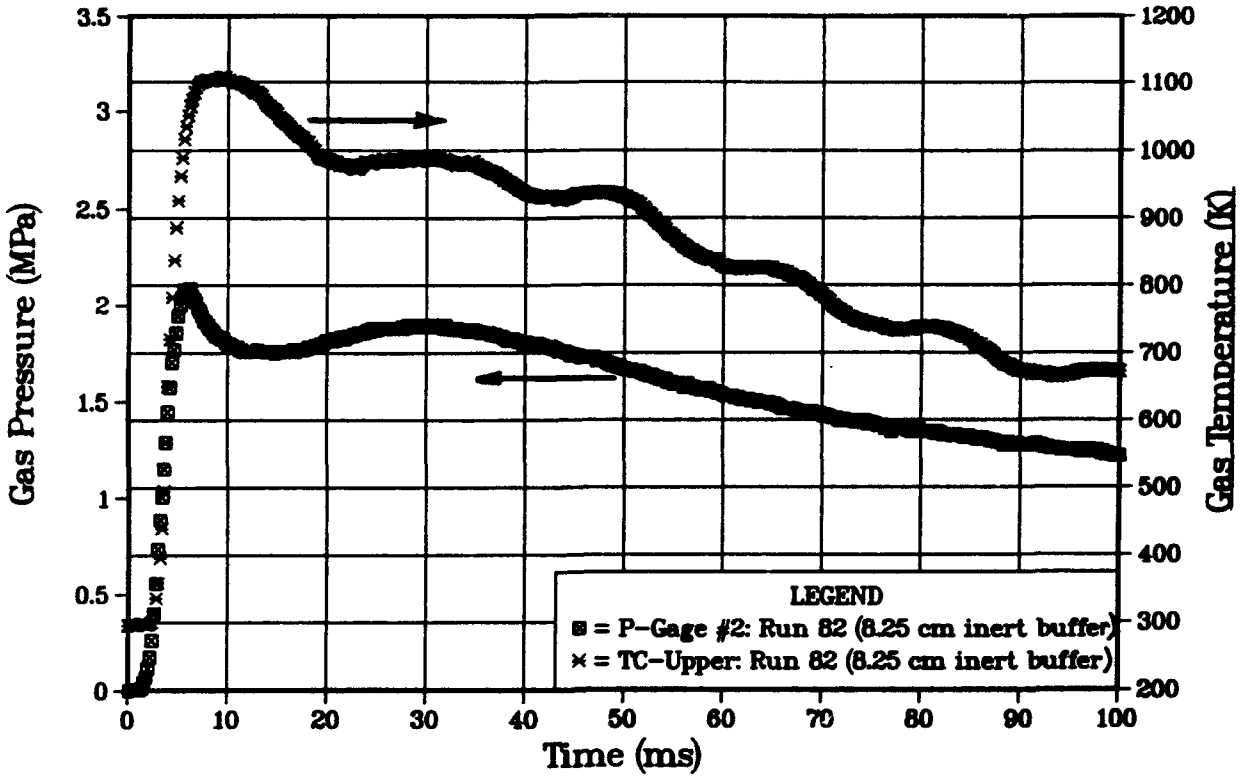

Figure 14. Comparison of temperature time-history from the 2-mil thermocouple and pressure time-history from the transducer at mid-chamber location P2. M43 propellant loaded into chamber with 82.5-mm inert buffer zone (Figure 10b).

3.3 Simulation with the XKTC Interior Ballistic Code. A future goal of this effort is to employ or develop a two-phase reactive flow model which can simulate the ignition and flamespreading behavior observed in the current experiment. A simple lumped-parameter (zero-dimensional) model of the dual chamber with bursting diaphragm was discussed in Kooker, Chang, and Howard (1992). Although the model was helpful in understanding the behavior of the diaphragm and nozzle-plate igniter system, it has no provision for the granular solid phase in the flow chamber, and it does not address any aspect of wave motion. Although upgrading this model is still an option, a modest attempt was made to use the XNOVAKTC Code (Gough 1990) which has enjoyed considerable success in various interior ballistics applications. Unfortunately, no easy way could be found to mimic the dual-chamber nature of the flamespreading apparatus, where a fine-grained solid begins burning in the sealed igniter chamber until reaching a burst pressure to start the nozzle flow. As a compromise, the current XKTC simulations ignore the igniter chamber (and nozzle plate) altogether and merely assume an igniter function at one end of the chamber containing the packed bed. Guided by results from the lumped-parameter model and experimental measurements, the XKTC igniter mass function was chosen to match typical pressure time-histories recorded by the three transducers in the chamber filled (except for 19 mm) with inert granular

simulant, subject to the constraint that 80% of the igniter mass (5 g total) is liberated in 3 ms. Clearly, uniqueness has been sacrificed here. A comparison with typical pressure transducer data is shown in Figure 15. No attempt was made to produce an exact match with these data since normal run-to-run variations in the igniter diaphragm burst process as well as loading the large grains into the chamber could account for these differences. Although the experimental pressurization event at P1 is only approximated here (the predicted overshoot character is similar to several other runs however), wave propagation through the compacted bed is predicted fairly well. Note also that the rate of pressure decay for time greater than 3.5 ms virtually parallels the experimental data, which seems to validate the code's description of heat loss to the granular bed and chamber walls. At this point, the properties of the igniter mass function were held fixed in all subsequent runs.

With this igniter function determined, an attempt was made to simulate the behavior of M30A1 granular propellant when confined in the full-up chamber configuration. Figure 16 is a plot of pressure time-history at the three gage locations (P1, P2, and P3), and compares experimental data with an XKTC prediction which assumes the same chamber configuration but *suppresses* ignition of the granular M30A1 propellant. Although the predictions at early time overshoot the experimental pressure data somewhat, the general behavior of the ignition wave is captured—including the pressure plateau level of 2 MPa. Note that the large-grain M30A1 forms a more permeable packed bed than the inert grains, which explains why the pressure plateau level decreases from that shown in Figure 15 (even though the igniter function is held fixed). The comparison in Figure 16 clearly shows that the pressure level beyond 7 ms is being augmented by some type of combustion process. The difficulty is that this "plateau-then-runaway" pressure behavior could not be simulated with XKTC operating under the usual assumptions, i.e., ignition occurs when the surface temperature of the propellant grain (heated as an inert solid) exceeds a threshold value, and the combustion process converts solid material directly to final products (no finite-rate chemistry) with full heat release. In fact, operating under these assumptions, there is a razor-thin boundary between successful ignition and failed ignition as illustrated by the two sets of pressure time-histories (at the three chamber gage locations) plotted in Figure 17. The code does not predict a response between these two extremes. Now of course, the actual propellant combustion process does proceed at some finite rate (as a result of competition among many rates), which is usually much faster than the concurrent flow processes. Thus, one possible conclusion from the comparison shown in Figure 16 and the predictions shown in Figure 17 is that, at these pressure levels, *the finite-rate process which controls heat release during transient combustion of M30A1 propellant is slow enough to be the rate-limiting event in this convective flow field.* At these same pressure levels, this would be equally true for M43 propellant whose flame structure includes a "dark zone" implying a finite-rate staged heat-release process.

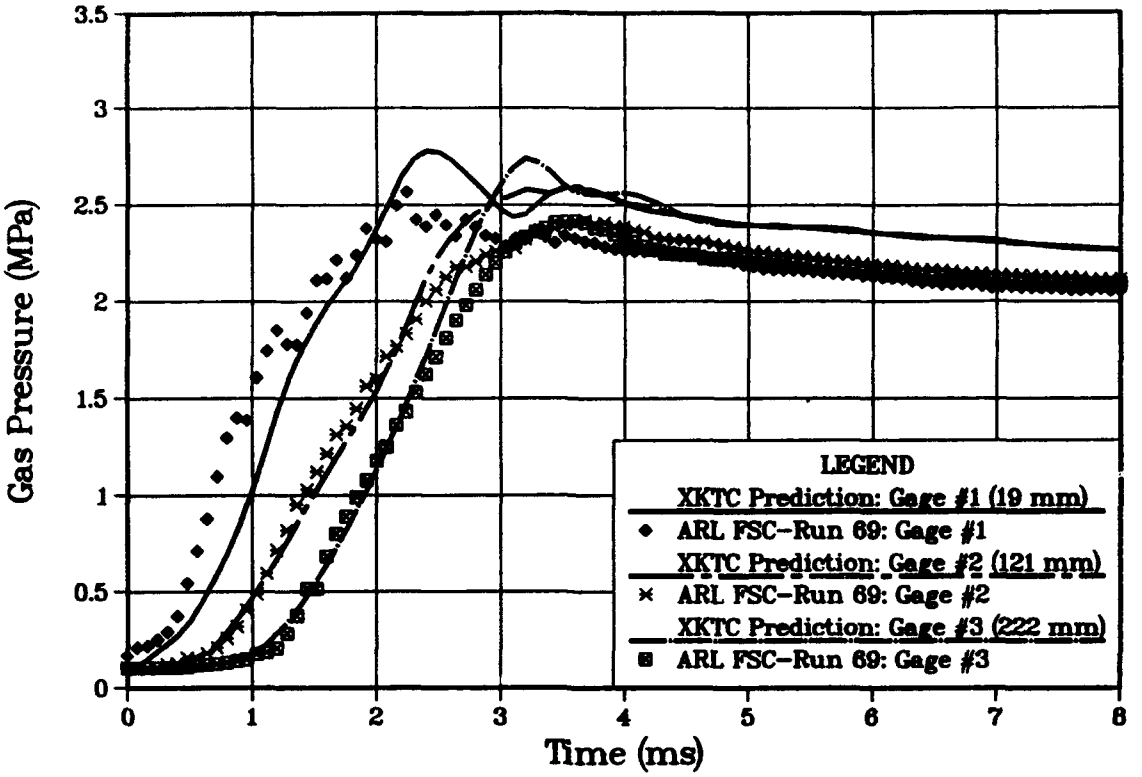

Figure 15. Comparison of pressure time-history at locations P1, P2, and P3 for the chamber loaded with inert granular simulant. Lines denote predictions from XNOVAKTC code.

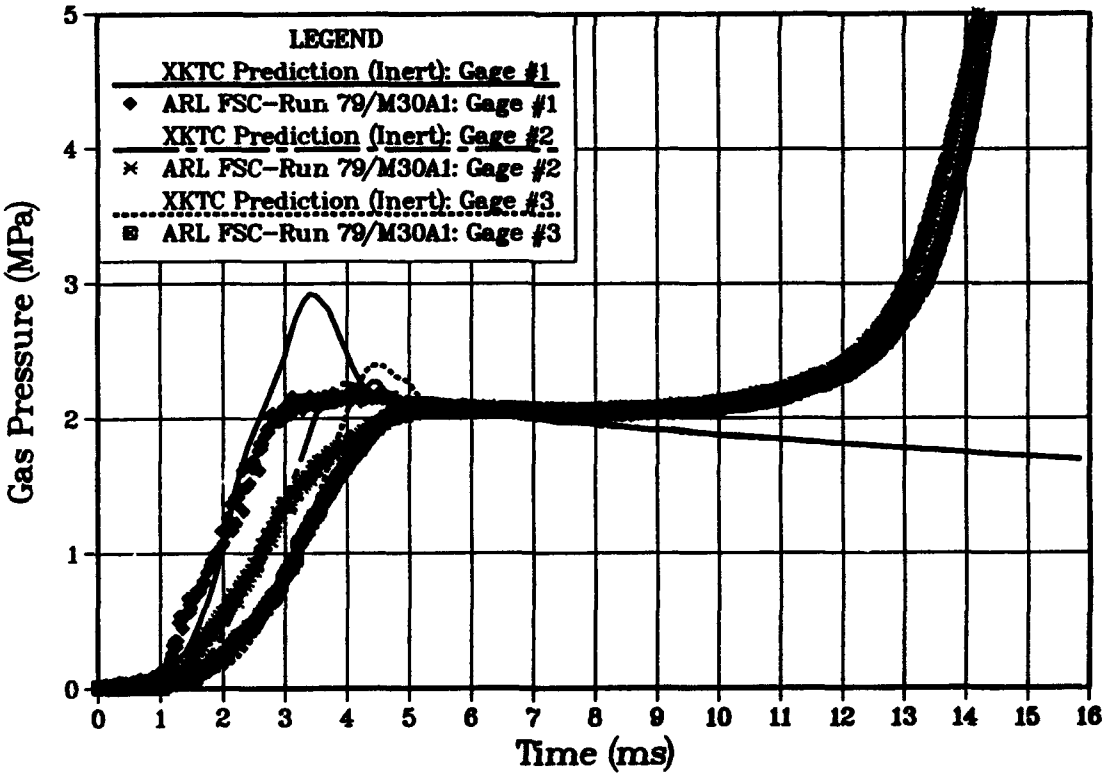

Figure 16. Comparison of pressure time-history at locations P1, P2, and P3 when chamber is loaded with M30A1 propellant in configuration of Figure 6a with no inert buffer zone. Curves are predictions from XNOVAKTC code with propellant ignition suppressed.

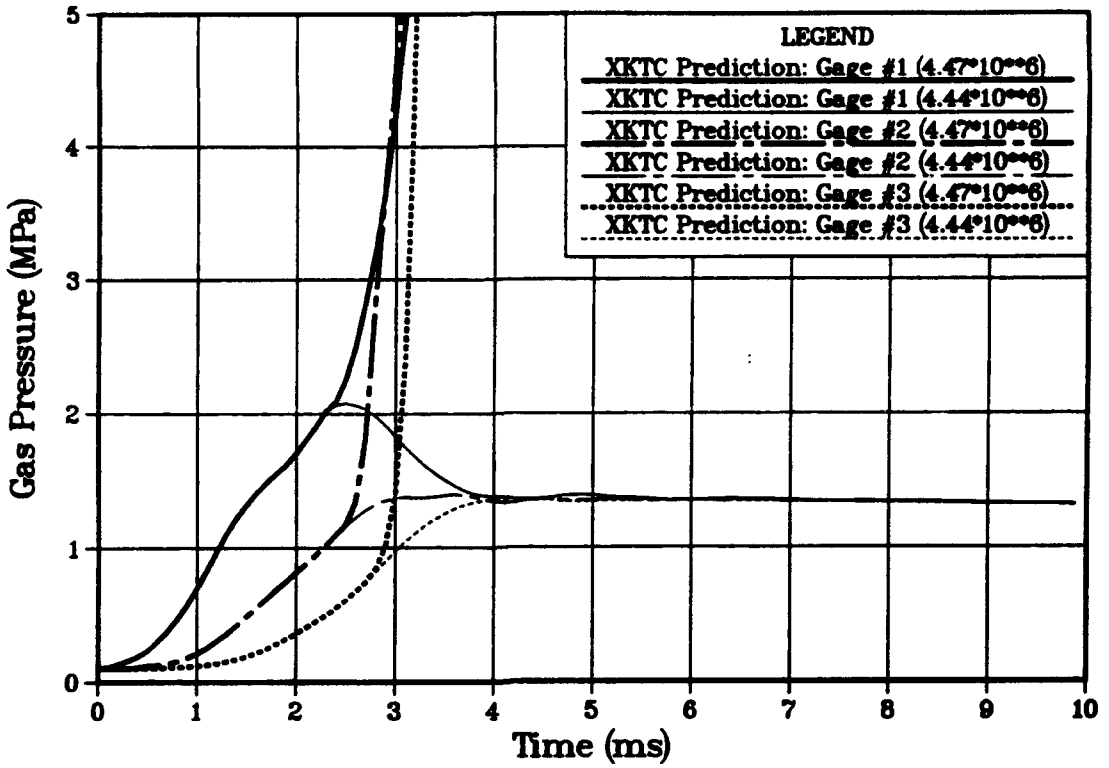

Figure 17. XNOVAKTC predictions for pressure time-history at locations P1, P2 and P3. Chamber loaded with M30A1 (no inert buffer zone). Ignition temperature threshold is 444 K. Bold curves imply successful ignition, light curves imply failed ignition. Difference in energy of igniter mass flux is 3 parts out of 447.

4. CONCLUDING REMARKS

The primary objective here was to develop a laboratory experiment capable of creating a controllable environment for studying the marginal convective ignition behavior of various solid gun propellants, particularly LOVA propellants. To help understand what happens during an anomalous ignition event in a granular propellant bed, the experiment measures both static pressure and temperature of the gases within the aggregate. The chamber apparatus is designed to generate a planar gas-phase wave to end-ignite a confined granular propellant column and then permit simultaneous monitoring of gas-phase pressure (with a series of wall-mounted transducers) and temperature (with fast-response thermocouples protected inside special steel holders protruding into the bed). A limited number of comparisons between 1-mil, 2-mil, and 3-mil Type S thermocouples suggest that the 1-mil should probably be adequate for the transient flowfield encountered here. However, in the current series of experiments, practical considerations forced the use of 2-mil thermocouples whose reported temperatures could be low by possibly 200 K during the initial 10-ms time interval. In general, the apparatus appears to be functioning as designed.

The igniter-driven wave has approximately a 3-ms rise time and, depending upon bed permeability, produces a gas pressure level of 2–3 MPa. Igniter strength in the dual-chamber experiment was held constant, but the influence of the hot-gas ignition wave could be modified by adjusting the length of an inert packed-bed buffer zone. Varying the length of this inert buffer zone causes both propellants to exhibit a "plateau-then-runaway" pressure time-history which closely mimics the "hang-fire" behavior observed by Chang & Rocchio (1988) in the 105mm gun simulator. Reproducing this behavior in a *controlled* experiment was an important objective here.

Results were obtained for two solid propellants, M30A1 and M43. The 7-perf cylindrical M30A1 grain is approximately twice the dimensions of the 19-perf cylindrical M43 LOVA grain; hence, the packed bed formed by the large-grain M30A1 is more permeable than that formed by the smaller grain M43. In the chamber configuration with no buffer zone, "insensitive" M43 propellant ignites more readily than M30A1 propellant. This fact serves to emphasize an important concept: *Time to ignition in a granular propellant bed is governed by competition between the "flow residence time" and the "characteristic time for chemical reaction"* (i.e., a Damkohler number). Although neither characteristic time is determined here, the current results demonstrate that flow environment adjustments that increase flow residence time and/or shorten the chemical reaction time will decrease the time to ignition. M43 provides a dramatic example; decreasing the length of the buffer zone causes time to ignition to change from infinity (i.e., ignition fails) to 40 ms to less than 2 ms. The "plateau-then-runaway" pressure time-history exhibited by both propellants cannot be simulated with the interior ballistics model (XKTC) assuming instantaneous conversion of reactive solid into gaseous products with full energy release. It is probable that, at these pressure levels, the finite-rate process that controls heat release during transient propellant combustion is slow enough to be the rate-limiting event in this convective flow field.

The experiment provided measurements of gas-phase temperature before the onset of full combustion. For the M30A1 propellant run which exhibits a 12–13 ms induction time, the mid-chamber thermocouple reports gas temperatures rising to 1,200 K and then increasing to 1,600 K before combustion runs away. For the M43 propellant run which exhibits a 40-ms induction time, gas temperatures at mid-chamber suggest a propellant contribution stimulated by the passage of the igniter-driven wave. The initial temperature pulse, however, is not sustained as values retreat into the range of 1,100 K to 800 K, but combustion eventually is successful.

With reference to M43, note that the gas temperatures monitored in this convective flow experiment during most of the 40ms-delay-case are near or just below the flame "dark zone" temperature [1200 K] measured by Teague, Singh and Vanderhoff (1993) [see Table 3 on page 10] in a strand-burner environment. The existence of a dark zone suggests a finite-rate staged heat-release process, which could become an additional liability during any attempt to establish a propellant flame zone in a convective flow. The fact that M43 fails to ignite under conditions when M30A1 is successful might be partially explained by the difference in flame-zone structure. Although conclusive proof is lacking, the temperature measurements and ignition behavior of M43 are consistent with the premise that the finite-rate process controlling energy release in the convective flow is actually that of the propellant "dark zone."

INTENTIONALLY LEFT BLANK.

5. REFERENCES

Chang, L-M., and J. J. Rocchio. "Simulator Diagnostics of the Early Phase Ignition Phenomena in a 105-mm Tank Gun Chamber." BRL-TR-2890, U.S. Army Ballistic Research Laboratory, Aberdeen Proving Ground, MD, March 1988.

Gough, P. S. "The XNOVAKTC Code." BRL-CR-627, U.S. Army Ballistic Research Laboratory, Aberdeen Proving Ground, MD, February 1990.

Horst, A. W. "Multiphase Flow Analysis of the Ballistic Performance of an Anomalous LOVA Propellant Mix." 20th JANNAF Combustion Meeting, CPIA Publication 383, vol. I, pp. 557-570, October 1983.

Howard, S. L., L-M. Chang, and D. E. Kooker. "Thermocouples for Interior Ballistic Temperature Measurement." ARL Report in preparation, 1994.

Kooker, D. E., L-M. Chang, and S. L. Howard. "An Attempt to Characterize Flamespreading in Granular Solid Propellant: Preliminary Results." 29th JANNAF Combustion Subcommittee Meeting, CPIA Publication 593, vol. I, pp. 1–13, October 1992. (See also Kooker, Chang, and Howard, "Flamespreading in Granular Solid Propellant: Design of an Experiment." ARL-MR-80, June 1993.)

Kuo, K. K., J. H. Koo, T. R. Davis, and G. R. Coates. "Transient Combustion in Mobile Gas-Permeable Propellants." Acta Astronautica, vol. 3, pp. 573–591, 1976.

Kuo, K. K., and J. H. Koo. "Transient Combustion in Granular Propellant Beds. Part I: Theoretical Modeling and Numerical Solution of Transient Combustion Processes in Mobile Granular Propellant Beds." Contract Report 346, U.S. Army Ballistic Research Laboratory, Aberdeen Proving Ground, MD, August 1977.

McClure, D. R. "Measurements of Gas Temperature and Convective Heat Flux in a Reacting Granular Propellant Bed." PhD Thesis, Department of Mechanical Engineering, The Pennsylvania State University, August 1984.

Miller, M. S. "Modeling of Kinetics and Combustion of Energetic Materials." ARO-URI Meeting on Fast Reaction Kinetics and Modeling of Energetic Material Combustion, The Pennsylvania State University, 6–7 August 1992.

Miller, M. S. Personal communications concerning extensive strand-burner experiments at the U.S. Army Research Laboratory, Aberdeen Proving Ground, MD, 1993.

Teague, M. W., G. Singh, and J. A. Vanderhoff. "Spectral Studies of Solid Propellant Combustion IV: Absorption and Burn Rate Results for M43, XM39, and M10 Propellants." ARL-TR-180, U.S. Army Research Laboratory, Aberdeen Proving Ground, MD, August 1993.

Vanderhoff, J. A., W. R. Anderson, and A. J. Kotlar. "Dark Zone Modeling of Solid Propellant Flames." 29th JANNAF Combustion Subcommittee Meeting, CPIA Publication 593, vol. II, pp. 225–237, October 1992.

INTENTIONALLY LEFT BLANK.

No. of Copies	Organization
2	Administrator Defense Technical Info Center ATTN: DTIC-DDA Cameron Station Alexandria, VA 22304-6145
1	Commander U.S. Army Materiel Command ATTN: AMCAM 5001 Eisenhower Ave. Alexandria, VA 22333-0001
1	Director U.S. Army Research Laboratory ATTN: AMSRL-OP-CI-AD, Tech Publishing 2800 Powder Mill Rd. Adelphi, MD 20783-1145
1	Director U.S. Army Research Laboratory ATTN: AMSRL-OP-CI-AD, Records Management 2800 Powder Mill Rd. Adelphi, MD 20783-1145
2	Commander U.S. Army Armament Research, Development, and Engineering Center ATTN: SMCAR-TDC Picatinny Arsenal, NJ 07806-5000
1	Director Benet Weapons Laboratory U.S. Army Armament Research, Development, and Engineering Center ATTN: SMCAR-CCB-TL Watervliet, NY 12189-4050
1	Director U.S. Army Advanced Systems Research and Analysis Office (ATCOM) ATTN: AMSAT-R-NR, M/S 219-1 Ames Research Center Moffett Field, CA 94035-1000

No. of Copies	Organization
1	Commander U.S. Army Missile Command ATTN: AMSMI-RD-CS-R (DOC) Redstone Arsenal, AL 35898-5010
1	Commander U.S. Army Tank-Automotive Command ATTN: AMSTA-JSK (Armor Eng. Br.) Warren, MI 48397-5000
1	Director U.S. Army TRADOC Analysis Command ATTN: ATRC-WSR White Sands Missile Range, NM 88002-5502
(Class. only) 1	Commandant U.S. Army Infantry School ATTN: ATSH-CD (Security Mgr.) Fort Benning, GA 31905-5660
(Unclass. only) 1	Commandant U.S. Army Infantry School ATTN: ATSH-WCB-O Fort Benning, GA 31905-5000
1	WL/MNOI Eglin AFB, FL 32542-5000
	Aberdeen Proving Ground
2	Dir, USAMSAA ATTN: AMXSY-D AMXSY-MP, H. Cohen
1	Cdr, USATECOM ATTN: AMSTE-TC
1	Dir, USAERDEC ATTN: SCBRD-RT
1	Cdr, USACBDCOM ATTN: AMSCB-CII
1	Dir, USARL ATTN: AMSRL-SL-I
5	Dir, USARL ATTN: AMSRL-OP-AP-L

1 HQDA (SAED-TR/Ms. K. Kominos)
WASH DC 20310-0103

1 HQDA (SARD-TR/Dr. R. Chait)
WASH DC 20310-0103

1 Chairman
DOD Explosives Safety Board
Room 856-C
Hoffman Bldg. 1
2461 Eisenhower Avenue
Alexandria, VA 22331-0600

1 Headquarters
U.S. Army Materiel Command
ATTN: AMCICP-AD, M. Fisette
5001 Eisenhower Ave.
Alexandria, VA 22333-0001

1 U.S. Army Ballistic Missile
Defense Systems Command
Advanced Technology Center
P.O. Box 1500
Huntsville, AL 35807-3801

1 Department of the Army
Office of the Product Manager
155mm Howitzer, M109A6, Paladin
ATTN: SFAE-AR-HIP-IP,
Mr. R. De Kleine
Picatinny Arsenal, NJ 07806-5000

2 Project Manager
Advanced Field Artillery System
ATTN: SFAE-ASM-AF-E,
LTC A. Ellis
T. Kuriata
Picatinny Arsenal, NJ 07801-5000

1 Project Manager
Advanced Field Artillery System
ATTN: SFAE-ASM-AF-Q, W. Warren
Picatinny Arsenal, NJ 07801-5000

1 Commander
Production Base Modernization Agency
U.S. Army Armament Research,
Development, and Engineering Center
ATTN: AMSMC-PBM, A. Siklosi
Picatinny Arsenal, NJ 07806-5000

1 Commander
Production Base Modernization Agency
U.S. Army Armament Research,
Development, and Engineering Center
ATTN: AMSMC-PBM-E, L. Laibson
Picatinny Arsenal, NJ 07806-5000

1 PEO-Armaments
Project Manager
Tank Main Armament System
ATTN: AMCPM-TMA
Picatinny Arsenal, NJ 07806-5000

1 PEO-Armaments
Project Manager
Tank Main Armament System
ATTN: AMCPM-TMA-105
Picatinny Arsenal, NJ 07806-5000

1 PEO-Armaments
Project Manager
Tank Main Armament System
ATTN: AMCPM-TMA-120
Picatinny Arsenal, NJ 07806-5000

1 PEO-Armaments
Project Manager
Tank Main Armament System
ATTN: AMCPM-TMA-AS, H. Yuen
Picatinny Arsenal, NJ 07806-5000

2 Commander
U.S. Army Armament Research,
Development, and Engineering Center
ATTN: SMCAR-CCH-V,
C. Mandala
E. Fennell
Picatinny Arsenal, NJ 07806-5000

1 Commander
U.S. Army Armament Research,
Development, and Engineering Center
ATTN: SMCAR-CCH-T, L. Rosendorf
Picatinny Arsenal, NJ 07806-5000

1 Commander
U.S. Army Armament Research,
Development, and Engineering Center
ATTN: SMCAR-CCS
Picatinny Arsenal, NJ 07806-5000

No. of Copies	Organization
1	Commander U.S. Army Armament Research, Development, and Engineering Center ATTN: SMCAR-AEE, J. Lannon Picatinny Arsenal, NJ 07806-5000
11	Commander U.S. Army Armament Research, Development, and Engineering Center ATTN: SMCAR-AEE-B, A. Beardell D. Downs S. Einstein S. Westley S. Bernstein J. Rutkowski B. Brodman P. O'Reilly R. Cirincione P. Hui J. O'Reilly Picatinny Arsenal, NJ 07806-5000
5	Commander U.S. Army Armament Research, Development, and Engineering Center ATTN: SMCAR-AEE-WW, M. Mezger J. Pinto D. Wiegand P. Lu C. Hu Picatinny Arsenal, NJ 07806-5000
3	Director Benet Laboratories ATTN: SMCAR-CCB-RA, G.P. O'Hara G.A. Pflegl SMCAR-CCB-S, F. Heiser Watervliet, NY 12189-4050
2	Commander U.S. Army Research Office ATTN: Technical Library D. Mann P.O. Box 12211 Research Triangle Park, NC 27709-2211
1	Commander, USACECOM R&D Technical Library ATTN: ASQNC-ELC-IS-L-R, Myer Center Fort Monmouth, NJ 07703-5301
1	Director HQ, TRAC RPD ATTN: ATCD-MA Fort Monroe, VA 23651-5143
1	Commander U.S. Army Belvoir Research and Development Center ATTN: STRBE-WC Fort Belvoir, VA 22060-5606
1	Director U.S. Army TRAC-Ft. Lee ATTN: ATRC-L, Mr. Cameron Fort Lee, VA 23801-6140
1	Commander Radford Army Ammunition Plant ATTN: SMCAR-QA/HI LIB Radford, VA 24141-0298
1	Commander U.S. Army Foreign Science and Technology Center ATTN: AMXST-MC-3 220 Seventh Street, NE Charlottesville, VA 22901-5396
2	Commander Naval Sea Systems Command ATTN: SEA 62R SEA 64 Washington, DC 20362-5101
1	Commander Naval Air Systems Command ATTN: AIR-954-Tech Library Washington, DC 20360
2	Commander Naval Research Laboratory ATTN: Technical Library Code 4410, E. Oran Washington, DC 20375-5000

No. of Copies	Organization
1	Office of Naval Research ATTN: Code 473, R.S. Miller 800 N. Quincy Street Arlington, VA 22217-9999
1	Office of Naval Technology ATTN: ONT-213, D. Siegel 800 N. Quincy St. Arlington, VA 22217-5000
2	Commander Naval Surface Warfare Center ATTN: Code 730 Code R-13, H. W. Sandusky 10901 New Hampshire Ave Silver Spring, MD 20903-5000
7	Commander Naval Surface Warfare Center ATTN: T.C. Smith K. Rice S. Mitchell S. Peters J. Consaga C. Gotzmer Technical Library Indian Head, MD 20640-5000
4	Commander Naval Surface Warfare Center ATTN: Code G30, Guns & Munitions Div Code G32, Guns Systems Div Code G33, T. Doran Code E23 Technical Library Dahlgren, VA 22448-5000
3	Commander Naval Air Warfare Center ATTN: Code 3891, C.F. Price A. Atwood Code 3895, Information Science Division China Lake, CA 93555-6001
1	Commanding Officer Naval Underwater Systems Center ATTN: Code 5B331, Technical Library Newport, RI 02840

No. of Copies	Organization
1	AFOSR/NA ATTN: J. Tishkoff Bolling AFB, D.C. 20332-6448
1	OLAC PL/TSTL ATTN: D. Shiplett Edwards AFB, CA 93523-5000
3	AL/LSCF ATTN: J. Levine L. Quinn T. Edwards Edwards AFB, CA 93523-5000
1	WL/MNAA ATTN: B. Simpson Eglin AFB, FL 32542-5434
1	WL/MNME Energetic Materials Branch 2306 Perimeter Rd. STE 9 Eglin AFB, FL 32542-5910
1	WL/MNSH ATTN: R. Drabczuk Eglin AFB, FL 32542-5434
2	NASA Langley Research Center ATTN: M.S. 408, W. Scallion D. Witcofski Hampton, VA 23605
1	Central Intelligence Agency Office of the Central References Dissemination Branch Room GE-47, HQS Washington, DC 20502
1	Central Intelligence Agency ATTN: J. Backofen NHB, Room 5N01 Washington, DC 20505
1	Director Sandia National Laboratories Energetic Materials & Fluid Mechanics Department, 1512 ATTN: M. Baer P.O. Box 5800 Albuquerque, NM 87185

No. of Copies	Organization
1	Director Sandia National Laboratories Combustion Research Facility ATTN: R. Carling Livermore, CA 94551-0469
1	Director Sandia National Laboratories ATTN: 8741, G. A. Beneditti P.O. Box 969 Livermore, CA 94551-0969
1	Director Lawrence Livermore National Laboratory ATTN: L-355, A. Buckingham P.O. Box 808 Livermore, CA 94550-0622
1	Director Los Alamos Scientific Lab ATTN: T3/D. Butler P.O. Box 1663 Los Alamos, NM 87544
2	Battelle ATTN: TWSTIAC V. Levin 505 King Avenue Columbus, OH 43201-2693
1	Battelle PNL ATTN: M. C. C. Bampton P.O. Box 999 Richland, WA 99352
1	Institute of Gas Technology ATTN: D. Gidaspow 3424 S. State Street Chicago, IL 60616-3896
1	Institute for Advanced Technology ATTN: T.M. Kiehne The University of Texas of Austin 4030-2 W. Braker Lane Austin, TX 78759-5329
2	CPIA - JHU ATTN: H. J. Hoffman T. Christian 10630 Little Patuxent Parkway Suite 202 Columbia, MD 21044-3200

No. of Copies	Organization
1	AFELM, The Rand Corporation ATTN: Library D 1700 Main Street Santa Monica, CA 90401-3297
1	Arrow Technology Associates, Inc. ATTN: W. Hathaway P.O. Box 4218 South Burlington, VT 05401-0042
1	AAI Corporation ATTN: J. Frankle P.O. Box 126 Hunt Valley, MD 21030-0126
2	Alliant Techsystems, Inc. ATTN: R.E. Tompkins J. Kennedy 7225 Northland Dr. Brooklyn Park, MN 55428
1	Textron Defense Systems ATTN: A. Patrick 2385 Revere Beach Parkway Everett, MA 02149
1	General Applied Sciences Lab ATTN: J. Erdos 77 Raynor Ave. Ronkonkama, NY 11779-6649
1	General Electric Company Tactical System Department ATTN: J. Mandzy 100 Plastics Ave. Pittsfield, MA 01201-3698
1	IITRI ATTN: M.J. Klein 10 W. 35th Street Chicago, IL 60616-3799
4	Hercules, Inc. Radford Army Ammunition Plant ATTN: L. Gizzi D.A. Worrell W.J. Worrell C. Chandler Radford, VA 24141-0299

No. of Copies	Organization
2	Hercules, Inc. Allegheny Ballistics Laboratory ATTN: William B. Walkup Thomas F. Farabaugh P.O. Box 210 Rocket Center, WV 26726
1	Hercules, Inc. Aerospace ATTN: R. Cartwright 100 Howard Blvd. Kenvil, NJ 07847
1	Hercules, Inc. Hercules Plaza ATTN: B.M. Riggleman Wilmington, DE 19894
1	MBR Research Inc. ATTN: Dr. Moshe Ben-Reuven 601 Ewing St., Suite C-22 Princeton, NJ 08540
1	Olin Corporation Badger Army Ammunition Plant ATTN: F.E. Wolf Baraboo, WI 53913
3	Olin Ordnance ATTN: E.J. Kirschke A.F. Gonzalez D.W. Worthington P.O. Box 222 St. Marks, FL 32355-0222
1	Olin Ordnance ATTN: H.A. McElroy 10101 9th Street, North St. Petersburg, FL 33716
1	Paul Gough Associates, Inc. ATTN: P.S. Gough 1048 South St. Portsmouth, NH 03801-5423
1	Physics International Library ATTN: H. Wayne Wampler P.O. Box 5010 San Leandro, CA 94577-0599

No. of Copies	Organization
1	Princeton Combustion Research Laboratories, Inc. ATTN: N.A. Messina Princeton Corporate Plaza 11 Deerpark Dr., Bldg IV, Suite 119 Monmouth Junction, NJ 08852
2	Rockwell International Rocketdyne Division ATTN: BA08, J. Flanagan R.B. Edelman 6633 Canoga Avenue Canoga Park, CA 91303-2703
2	Rockwell International Science Center ATTN: Dr. S. Chakravarthy Dr. S. Palaniswamy 1049 Camino Dos Rios P.O. Box 1085 Thousand Oaks, CA 91360
1	Science Applications International Corp. ATTN: M. Palmer 2109 Air Park Rd. Albuquerque, NM 87106
1	Southwest Research Institute ATTN: J.P. Riegel 6220 Culebra Road P.O. Drawer 28510 San Antonio, TX 78228-0510
1	Sverdrup Technology, Inc. ATTN: Dr. John Deur 2001 Aerospace Parkway Brook Park, OH 44142
3	Thiokol Corporation Elkton Division ATTN: R. Willer R. Biddle Tech Library P.O. Box 241 Elkton, MD 21921-0241
1	Veritay Technology, Inc. ATTN: E. Fisher 4845 Millersport Hwy. East Amherst, NY 14501-0305

No. of Copies	Organization
1	Universal Propulsion Company ATTN: H.J. McSpadden 25401 North Central Ave. Phoenix, AZ 85027-7837
1	SRI International Propulsion Sciences Division ATTN: Tech Library 333 Ravenwood Avenue Menlo Park, CA 94025-3493
	Aberdeen Proving Ground
1	Cdr, USACSTA ATTN: STECS-PO/R. Hendricksen

INTENTIONALLY LEFT BLANK.

USER EVALUATION SHEET/CHANGE OF ADDRESS

This Laboratory undertakes a continuing effort to improve the quality of the reports it publishes. Your comments/answers to the items/questions below will aid us in our efforts.

1. ARL Report Number ARL-TR-446 Date of Report June 1994

2. Date Report Received _____

3. Does this report satisfy a need? (Comment on purpose, related project, or other area of interest for which the report will be used.) _____

4. Specifically, how is the report being used? (Information source, design data, procedure, source of ideas, etc.) _____

5. Has the information in this report led to any quantitative savings as far as man-hours or dollars saved, operating costs avoided, or efficiencies achieved, etc? If so, please elaborate. _____

6. General Comments. What do you think should be changed to improve future reports? (Indicate changes to organization, technical content, format, etc.) _____

CURRENT ADDRESS

_____
Organization

_____
Name

_____
Street or P.O. Box No.

_____
City, State, Zip Code

7. If indicating a Change of Address or Address Correction, please provide the Current or Correct address above and the Old or Incorrect address below.

OLD ADDRESS

_____
Organization

_____
Name

_____
Street or P.O. Box No.

_____
City, State, Zip Code

(Remove this sheet, fold as indicated, tape closed, and mail.)
(DO NOT STAPLE)

DEPARTMENT OF THE ARMY

OFFICIAL BUSINESS

BUSINESS REPLY MAIL
FIRST CLASS PERMIT No 0001, APG, MD

Postage will be paid by addressee.

Director
U.S. Army Research Laboratory
ATTN: AMSRL-OP-CI-B (Tech Lib)
Aberdeen Proving Ground, MD 21005-5066

NO POSTAGE
NECESSARY
IF MAILED
IN THE
UNITED STATE